# Copyright Warning & Restrictions

The copyright law of the United States (Title 17, United States Code) governs the making of photocopies or other reproductions of copyrighted material.

Under certain conditions specified in the law, libraries and archives are authorized to furnish a photocopy or other reproduction. One of these specified conditions is that the photocopy or reproduction is not to be "used for any purpose other than private study, scholarship, or research." If a, user makes a request for, or later uses, a photocopy or reproduction for purposes in excess of "fair use" that user may be liable for copyright infringement,

This institution reserves the right to refuse to accept a copying order if, in its judgment, fulfillment of the order would involve violation of copyright law.

Please Note: The author retains the copyright while the New Jersey Institute of Technology reserves the right to distribute this thesis or dissertation

Printing note: If you do not wish to print this page, then select "Pages from: first page # to: last page #" on the print dialog screen

# ABSTRACT

Weakness of inspiratory muscles is a major cause of respiratory failure. There are many clinical circumstances in which it may occur. The diaphragm is a major respiratory muscle. It has been difficult to quantify its shape, curvature and length.

To solve this question, a three dimensional diaphragm equation was derived on the assumption that the diaphragm is only attached at its periphery to the rib cage and the abdomen is filled with fluid. Computer programs were developed to fit the equation to the diaphragm contours obtained from plane X rays.

The results indicate that the ratio of transdiaphragmatic pressure to the surface tension of the diaphragm is relatively independent of lung volume, which supports the previous finding that the force-length relation is a more important geometric factor in diaphragm mechanics. Comparing the diaphragm contour of the normal person to two patients with ascites, it is suggested that the ascites patients have higher transdiaphragmatic pressure than normal patients.

# THREE DIMENSIONAL DIAPHRAGM SIMULATION MODEL FOR THE RELATIONSHIP OF THE TENSION, PRESSURE AND SHAPE

by
Zhangming He

A Thesis
Submitted to the Faculty of
New Jersey Institute of Technology
in Partial Fulfillment of the Requirements for the Degree of
Master of Science in Biomedical Engineering

Biomedical Engineering Committee

January 1994

APPROVAL PAGE

# THREE DIMENSIONAL DIAPHRAGM SIMULATION MODEL FOR THE RELATIONSHIP OF THE TENSION, PRESSURE AND SHAPE

Zhangming He

Dr. Peter Engler, Thesis Advisor — Date
Associate Professor of Electrical Engineering, NJIT

Dr. David Kristol, Committee Member — Date
Director and Professor of Biomedical Engineering, NJIT

Dr. A. Ritter, Committee Member — Date
Professor of Physiology, UMDNJ

# BIOGRAPHICAL SKETCH

**Author:** Zhangming He

**Degree:** Master of Science in Biomedical Engineering

**Date:** January 1994

**Undergraduate and Graduate Education:**

- Master of Science in Biomedical Engineering,
  New Jersey Institute of Technology
  Newark,New Jersey,1994

- Bachelor of Engineering in Biomedical Engineering,
  Shanghai Medical University,Shanghai,China,1985

**Major:** Biomedical Engineering

## ACKNOWLEDGMENTS

I would like to express my sincere gratitude to my thesis advisor, Dr. Engler, for his outstanding support and expert guidance to my research and thesis work. His comments and assistance always showed me the right way to complete the thesis.

My special thank to Dr. David Kristol, for his support and encouragement. His advice and help were the basis of my education in NJIT.

I thank Dr. R. Ritter who gave me important and detailed advice for the simulation model. I thank Dr. Lavietes who gave me guidance in medicine and offered the X-ray films. Their important advice was always there when I needed them.

I am indebted to my wife, Huimin Zhen, who contributed a lot to the thesis, including moral encouragement, useful discussion and typing.

## TABLE OF CONTENTS

LIST OF FIGURES

LIST OF FIGURES
(Continued)

LIST OF FIGURES
(Continued)

Figure Page

# CHAPTER 1

# INTRODUCTION

## 1.1 Physiological View

Agostoni et al. (1) suggested the concept that there were two pathways for lung volume displacement, one via the rib cage and one via the diaphragm-abdomen pathway. The diaphragm plays a very important role in respiration.

Normal inspiration is produced principally by the contraction of the diaphragm. Other muscles of inspiration are external intercostals, erectus muscles of the spine, and scapular elevators plus anterior serrati scaleni. The muscle of diaphragm is bell shaped so that contraction of any of its muscle fibers pulls it downward to cause inspiration ie, the contraction of the diaphragm lowers the dome.

The diaphragm is innervated by the phrenic nerves. These originate at the third, fourth, and fifth cervical levels, where they synapse with axons from cell bodies in the medulla. The external intercostals are also innervated by fibers that synapse with axons from the medulla. For most inspiratory demands, contraction of the diaphragm and the intercostals, which elevate the ribs, suffices. However, during great inspiratory effort, the scaleus and the pectoralis minor muscles contribute by raising the rib cage and expanding the circumference of the chest cavity.

Ordinarily, expiration is an entirely passive process; that is, when the diaphragm relaxes, the elastic structures of the lung, chest cage, and abdomen, as well as the tone of the abdominal muscles, force the diaphragm upward. However, if forceful expiration is required, the diaphragm can also be pushed upward powerfully by active contraction of the abdominal muscles against the abdominal contents. Thus, all the abdominal muscles combined represent the major muscles of expiration.

Normal pulmonary ventilation is accomplished almost entirely by the muscles of inspiration. On relaxation of the inspiratory muscle the elastic properties of the lungs and thorax cause the lungs to contract passively. Weakness of inspiratory muscles is a major cause of respiratory failure. There are many clinical circumstances in which this may occur.

The diaphragm is the major inspiratory muscle with its curved and three dimensional shape. Its ability to generate inspiratory force depends upon at least three variables: 1, length; 2, curvature; and 3, its position relative to the rib cage.

**1.2 Historical View**

The relationships between the diaphragmatic muscle length, contractile tension, and transdiaphragmatic pressure have been determined by direct measurement in the open-chest dog(2). Braun et al.(3) have studied the force-length

relationship of the human diaphragm. To characterize the in-vivo force-length relationship of the human diaphragm, they related pressures during static inspiratory efforts, respiratory muscle pressure (Pmus) and transdiaphragmatic pressures (Pdi) respectively to diaphragm lengths measured on chest X rays from 22 normal subjects. They found that the diaphragm length-lung volume relation is curvelinear, with length increasing primarily in the proportion to the length of the part of the diaphragm which attaches to the chest wall. As length increased, Pmus and Pdi rise sharply then plateau, generally conforming to force-length behavior of isolated muscle.

The causes that affect the curvature and length of the diaphragm are very complicated. Loring et al.(4) used X-rays, ultrasound, and linear measurements of thoracic and abdominal diameters to estimate the relationships between lung volume, thoracoabdominal configuration and diaphragmatic lengths, and they found that diaphragmatic length are strongly coupled to both rib cage dimensions as well as abdominal PA dimension.

These studies contributed a lot to the concepts of the mechanics of the diaphragm. But all this research was restricted to measurement and statistics and offered no mathematical theory or validation for these measurements. In 1983, Whitelaw et al(5) established a mathematical model to describe the relationship between pressure, tension, and shape of the diaphragm. Using this model, the shape of the

diaphragm dome was calculated from transdiaphragmatic pressure and tension in the diaphragm.

When the author of this thesis tried to use this model to study the diaphragm curves, it was found that there were some mistakes in this model.

In this thesis, the simulation model of the diaphragm was derived to meet the needs to study the mechanics of the diaphragm.

# CHAPTER 2

## DERIVATION OF THE SHAPE EQUATION OF DIAPHRAGM

To obtain the shape equation of the diaphragm shape, it was assumed that the muscle acts as a free membrane,attached at its edges to the inside of a vertical rib cage that is circular in cross section, that the attachments are inferior to the point at which the dome makes contact with the rib cage,and the abdomen is filled with fluid with a hydrostatic gradient in pressure(6).

### 2.1 THE LAW OF LAPLACE

For any membrane under tension,the force balance between transmembrane pressure,and tension is given by a generalized form of the "law of laplace",namely

$$P=T\left(\frac{1}{r1}+\frac{1}{r2}\right) \qquad (1)$$

Where r1(cm) and r2(cm) are the two principal radii of curvature, measured in orthogonal planes. $P(N/cm^2)$ is the transdiaphragmatic pressure, which is equal to abdominal pressure minus pleural pressure; i.e., P=Pab - Ppl. Pab is the pressure in the abdomen, Ppl is the pleural pressure and T(N/cm) is the tension of the diaphragm. As the muscle contracts, tension increases and the dome descends.

(Facing 7)

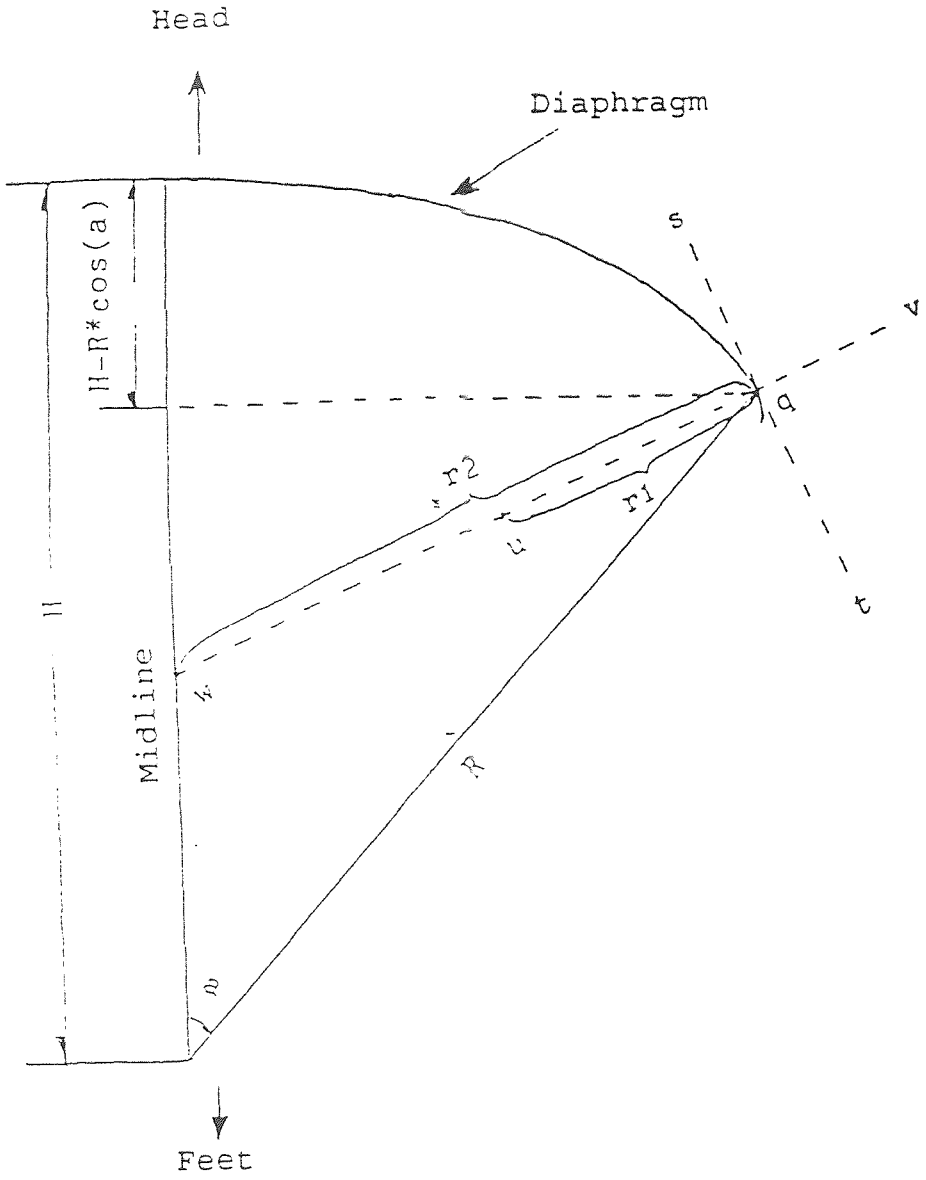


Figure 2.1 Radii of curvature.

The surface of the diaphragm is defined by the function R(a,b). Any point is described by its distance R from the origin and the "elevation" angle a and the "azimuth" angle b, as show in Fig. 2.1 and Fig. 2.2. In figure 1, at point q a line sqt is drawn tangent to the surface in the plane of the page. The curvature in the plane of the page is given by r1 on the line perpendicular to the tangent line(line vqw) and the corresponding center of curvature is at point u (Fig.2.1). The curvature in the plane perpendicular to the page and passing through the line sqt is given by the other principal radius of curvature, r2, and the corresponding center of curvature lies at point w. (This have been described in (5) and verified in page 335 of (6))

## 2.2 THE PRINCIPLE RADII OF CURVATURE

According to the definition, at a point P on a regular curve C,the curvature K, of C is the absolute value of rate of change of the direction angle W of the tangent with respect to distance on C in Figure 2.3

$$K=\frac{dw}{ds} \qquad (2)$$

The radius of curvature R is defined as the reciprocal of the curvature(7)

$$r=\frac{1}{K} \qquad (3)$$

The largest and the smallest radii at the point P are called the principle radii of curvature of point P.

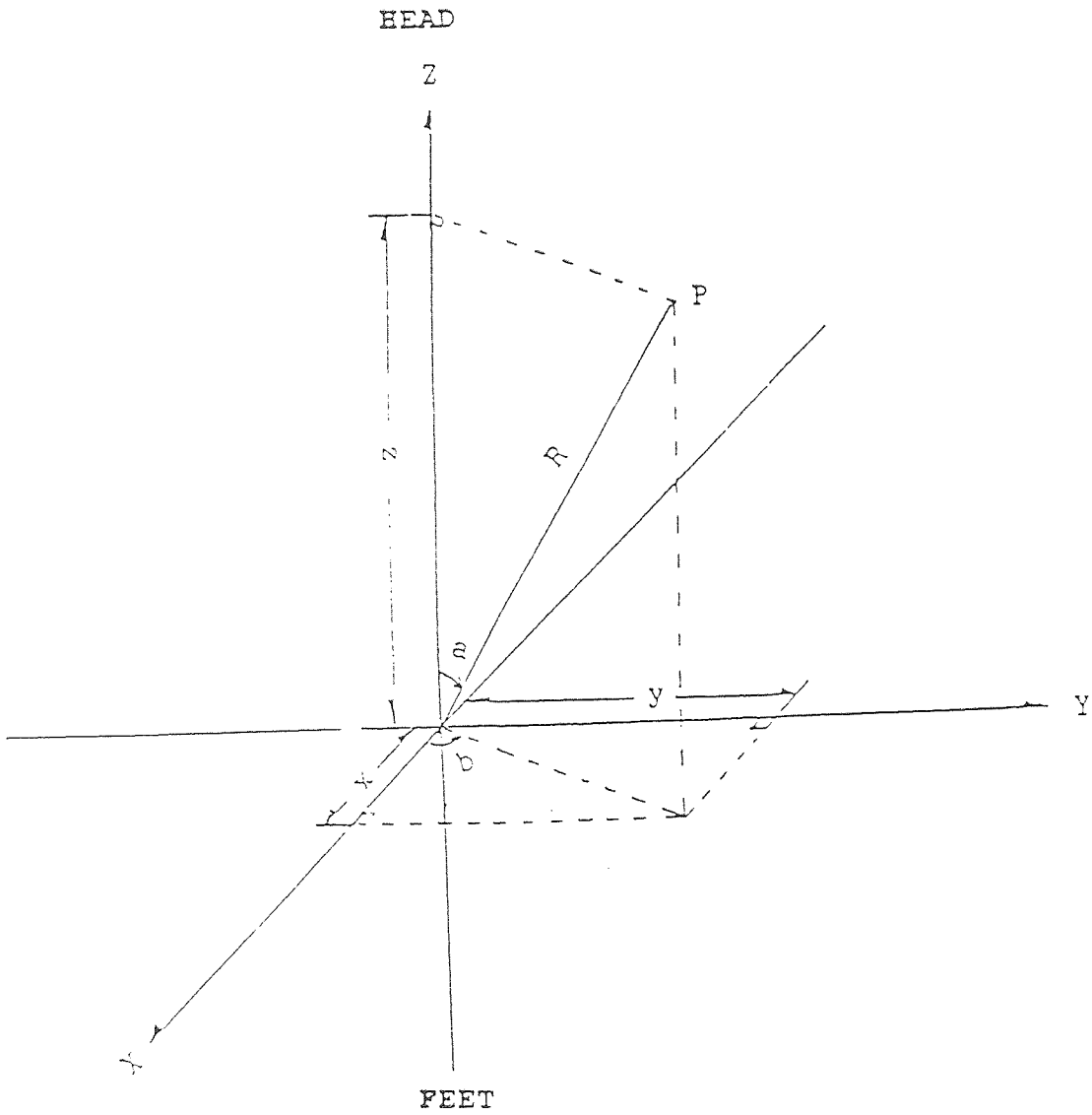


Figure 2.2 The point of diaphragm surface in three dimensions.

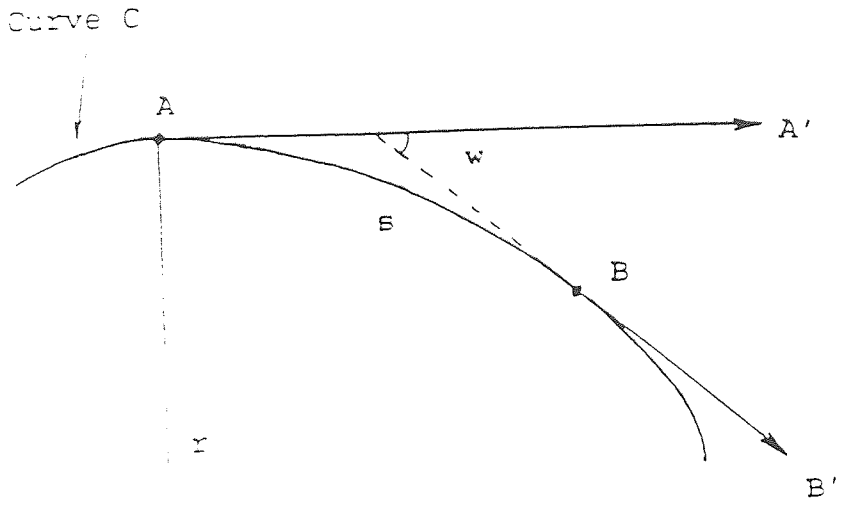


Figure 2.3 Definition of cuvature K. K equal to 1/r. r is the principle radius. AA' and BB' are the tangent lines at point A and B. w is the angle between lines AA' and BB'. s is the distance between point A and B.

If, in a three dimension rectilinear coordinate system, a surface defined by $f(x,y,z)=0$ and $x,y,z$ are determined by two angles a and b in Figure 2, the principle radii can be calculated by the equation

$$Ar^2+Br+C=0 \qquad (4)$$

Where the solutions r1 and r2 of equation (4) are the principle radii and

$$A=E'G'-F'^2; \qquad (5)$$

$$B=-H(G'E'+GE'-2FF'); \qquad (6)$$

$$C=H^4; \qquad (7)$$

$$E=x_a^2+y_a^2+z_a^2; \qquad (8)$$

$$F=x_a x_b+y_a y_b+z_a z_b; \qquad (9)$$

$$G=x_b^2+y_b^2+z_b^2; \qquad (10)$$

$$H=EG-F^2; \qquad (11)$$

$$E'=\begin{vmatrix} x_{aa} & y_{aa} & z_{aa} \\ x_a & y_a & z_a \\ x_{ab} & y_{ab} & z_{ab} \end{vmatrix} \qquad (12)$$

$$F'=\begin{vmatrix} x_{ab} & y_{ab} & z_{ab} \\ x_a & y_a & z_a \\ x_b & y_b & z_b \end{vmatrix} \qquad (13)$$

$$G'=\begin{vmatrix} x_{bb} & y_{bb} & z_{bb} \\ x_a & y_a & z_a \\ x_b & y_b & z_b \end{vmatrix} \qquad (14)$$

$x_a, y_a, z_a$, et al are the partial derivatives of $x,y,z$ relative to a and b(7).

## 2.3 THE SHAPE EQUATION OF DIAPHRAGM

Substituting r1 and r2 in the Laplace law, equation(1) (please find the derive of r1 and r2 in Appendix B), we have

$$\frac{P}{T} = \frac{2(R')^2+R^2-RR''}{[R^2+(R')^2]^{3/2}} + \frac{1-(R'/R)\cot(a)}{[R^2+(R')^2]^{1/2}} \quad (15)$$

Solving for RR"

$$RR''=2(R')^2+R^2+[1-(R'/R)\cot(a)][R^2+(R')^2] - \frac{P}{T}[R^2+(R')^2]^{3/2} \quad (16)$$

Substituting $P=P0+\rho gh$ and $h=H-R\cos(a)$ in equation(16), where $\rho$ is the density coefficient of the abdominal fluid, g is the gravitation coefficient, H is the distance from the top of the dome to the origin (refer to Figure 1.1). we get

$$R''=2R+\frac{3(R')^2}{R} - \frac{R'\cot(a)[R^2+(R')^2]}{R^2} - \frac{1}{T}\left[\frac{P0+\rho gH}{R} - \rho g\cos(a)\right]*[R^2+(R')^2]^{3/2} \quad (17)$$

Equation (17) is the shape equation of diaphragm. It is different from Whitelaw's equation in the sign between the 2nd and 3rd terms, and the denominators of the second and third terms.

$$R''=2R+\frac{3(R')^2}{R'}+\frac{R'}{R^2,}\cot(a)*[R^2+R')^2]$$

$$-\frac{1}{T}*[\frac{P0+\rho gH}{R}-\rho g\cos(a)]*[R^2+(R')^2]^{3/2}$$

In a personal contact with Dr. Whitelaw, he clarified that an associate developed the equation and he was unable to explain the discrepancy(16).

# CHAPTER 3

# PROGRAMS DEVELOPED TO PROCESS CURVES USING DIAPHRAGM EQUATION

## 3.1 About the MATLAB

MATLAB was originally written to provide easy access to matrix software developed by the LINPACK and EISPACK projects. It is a high-performance interactive software package for scientific and engineering numeric computation. MATLAB integrates numerical analysis, matrix computation, and graphics in an easy-to-use environment. It supplies the users flexible and programmable ways to process differential equation and curve analysis. These are why the author of this thesis chose it as the major software to develop the diaphragm model.

MATLAB is usually used in a command-driven mode; when single-line commands are entered, MATLAB processes them immediately and displays the results. It also has a strong function to execute sequences of commands that are stored in files. Disk files that contain MATLAB statements are called M-file. The following programs are edited in the M-files.

## 3.2 HBU.M Representing the Diaphragm Equation

A function in MATLAB used to present the diaphragm equation is ODE23, which integrates a system of ordinary differential equations using 2nd and 3rd order Runge-Kutta formulas. In

ODE23 it is necessary to have an equation representing M-file. HBU.M is the M-file to represent diaphragm equation(16) which is showed as follow:

```
% function to represent the diaphragm equation
% t, x are the input supplied by the ODE23
% x(1)=x'(t), x(2)=x(t)
% xdot is the output matrix of the function to ODE23.
function xdot=hbu(t,x)
a=x(2).*2.0+3.0*x(1).^2/x(2);
b=x(1).*(x(1).^2+x(2).^2);
c=x(2).^2*tan(t*pi/180.0);
d=(x(1).^2+x(2).^2).^1.5;
e=((te*2.0/r0+ru*980.0*r0)/x(2)...
   -ru*980.0*cos(t*pi/180.0))/te
xdot(1)=a-b/c-d*e;
xdot(2)=x(1);
% xdot(1)=x"(t), xdot(2)=x'(t)
```

In this M-file, x is the radius R in Figure 2.1; t is the angle a in Figure2.1; ru is the density of the fluid under the diaphragm, which is $\rho$ in equation(16); te is the tension of the diaphragm, which is T in equation(16); r0 is the radius when the "elevation" angle a in Figure 1 equal to zero.

### 3.3 BB.M Integrating and Plotting the Diaphragm Curve

This M-file use the ODE23 to integrate the diaphragm equation and plot out the result. (Refer BB.M in appendix C)

### 3.4 M.M Obtaining the Mid Point of X-ray Data Became Zero

To compare the measured(traced) contour of the diaphragm with the mathematically derived contour( Equation 17), it is necessary that the two curves be compared at the same coordinate scales. To this end the two curve are scaled so that the start and end points have the same x coordinates, and the mid point of the measured curve is positioned at y=0 (Figure 3.1).

```
%Shifting the middle point of d to zero
dm=mean(d);
% dm=the mean value of the x-ray curve.
d(:,2)=d(:,2)-dm;
clear dm
```

### 3.5 ZH.M Fitting the Curve with the X-ray Film Data

ZH.M (Refer ZH.M in Appendix D and Figure 3.1) is a M-file that shifts the calculated curve to overlap the measured(traced) curve. It functions to scale the measured curve such that the beginning and the end points of the

measured and calculated curves have the same x coordinates, and that the mid point of the curve crosses the x axis (y=0). The program then calculates the mean of the square of the difference in the y coordinates of the two curves.

$$sf=(y_{meas}-y_{calc})^2/N$$

sf is used to measure the goodness of the fit between the two curves. N is the number of the points in each curve. The length of the diaphragm model and the area under the diaphragm are also calculated in the ZH.M.

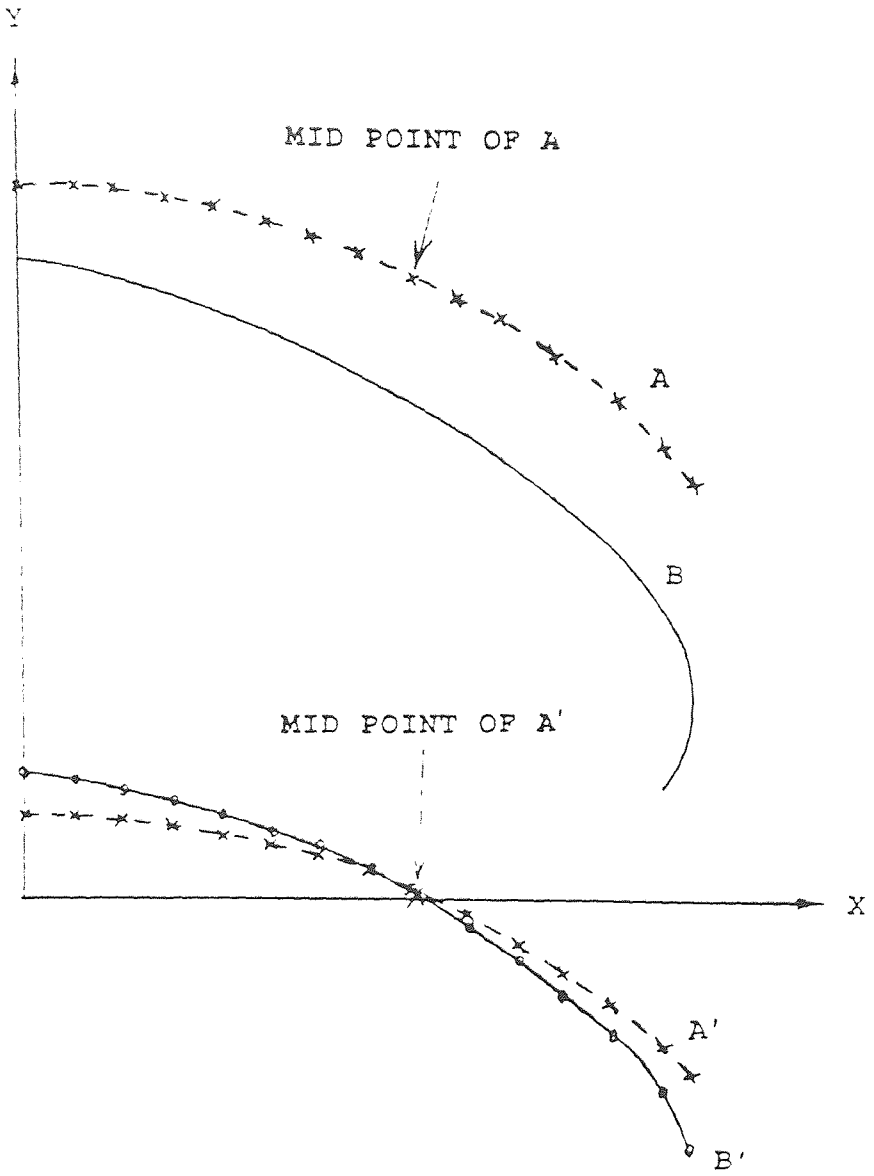


Figure 3.1 To make the measured (traced) curve A and the calculated curve B comparable, M.M shifts curve A to A' where the mid point of the curve crosses the x axis (y=0); ZH.M shifts the calculated curve B to B' such that A' and B' have the same x values at the begining and end points.

# CHAPTER 4

## RESULTS FROM MATHEMATICAL MODEL

Figure A.1 to A.6 show the calculated curves with the curvature equal to 11cm at the top of the dome. The model equation was solved by starting at an angle equal to 0.001 degree and applying the Runge-Kutta method.

The 2nd and 3rd Runge-Kutta method is the scheme to integrate from one point(t) to next point(t+t1). The compution procedure was carefully arranged as

$$R(t+t1)=R(t)+t1*(R'(t)+4*R'(t+t1/2)+R'(t+t1))/6$$

$$R'(t+t1)=R'(t)+t1*(R''(t)+4*R''(t+t1/2)+R''(t+t1))/6$$

R"(t) was calculated by the equation (17).

Figure A.1, A.3 and A.5 shows the simulate curve in polar coordinates. The lower solid lines are the derivative of radius R with respect to the angle a (Figure 2.1). The upper dotted lines show the radius against the angle a. The radius decreases when the angle increases.

Fig A.2, A.4 and A.6 shows the model curves in the rectlinear coordinate system for different tension values te. With the same radius of curvature at the top of the dome, r0=11cm, the shape of the curve changes as tension te changes.

In the beginning, the initial conditions were choosen as R'(0.001)=0, R"(0.001)=0. It was found that changing the value of R'(0.001) from 0 to $-1*10^{-5}$ will not significantly

change the result. The radius of curvature r0 and surface tension coefficient are the two parameters which can be arbitrarily assigned. The transdiaphramatic pressure at the apex is determined by the boundary condition

$$P=2*Te/r0$$

Figure A.7 to A.15 show the families of solutions to mathematical model with the same radius of curvature at the apex but different tensions. The range of radius of curvature at the apex varies from 6 to 60 cm. The surface tension coefficient varies from 0.05 to 10N/cm, which is sufficient to cover the range of the shapes of the human diaphragm. When the radius of curvature at the top of the dome was fixed, the shape of the simulated curve significantly changed with the change in surface tension. It is evident from the curves that the larger the radius of the rib cage is, the more tension is needed to maintain the contour of the diaphragm which forms a tangent to the vertical rib cage. It means the larger the diaphragm size is, the larger the tension is needed to sustain the shape of diaphragm. This result is independent with change of the curvature radius at the apex.

Figure A.16 to A.19 are the curves of the ratio of diaphragmatic pressure to surface tension P/Te against P. It can be seen in these graphs that the changes of P/Te is small when P is greater than about 0.3 N/cm. Because the abdominal pressure Pab changes very little, the changes in P=Pab-Ppl is nearly equal to the changes of Ppl(pleural

pressure). The lung compliance is also nearly constant in this region of the pressure-volume curve, so that the changes in pleural pressure Ppl are approximate proportional to the changes in lung volume. We therefore deduce that when the lung volume increases, the changes of the ratio of transdiaphragmatic pressure to surface tension is small.

Figure A.20 to A.22 shows best fitting curve for two ascites patients and a normal person.

Ascites is a reflection of changes in colloidal osmotic pressure within the fluid vessels (including the lymphatics) draining the peritoneal cavity. In this case, the diaphragm of ascites patient is quite like the simulated model that assumes the abdomen is filled with fluid.

In the thesis the mathematical model was applied to two patients with ascites, and one normal patient. In order to obtain the best fit of the mathematical model of the diaphragm contour to the contour measured by conventional X ray, the surface tension Te were 4.5 and 3.5 N/cm for the ascites models and 3.35 N/cm for the normal model (Fig A.20-A.22). These values do not differ significantly. Consequently it is concluded that it is the transdiaphragmatic pressure which is significantly higher in the ascites cases related to the normal case.

The length of diaphragm were 13.30 and 13.31 cm for the ascites models and 11.59 cm for the normal model. The area under diaphragm are 55.45 and 55.63 $cm^2$ for the ascites models and 40.97 $cm^2$ for the normal model.

# CHAPTER 5

## CONCLUSION AND DISCUSSION

A three dimensional mathematical diaphragm model is established. The shape of the diaphragm dome is determined by the transdiaphragmatic pressure and tension in the diaphragm.

The model is based on the following assumption:

(1) The diaphragm acts like a free membrane attached to therib cage. It offers no resistance to bending and distortion but supports tension.

(2) The diaphragm is attached to the lower borders of the rib cage at its edges.

(3) The ligaments, which attach the diaphragm to the pericardium and liver, are assumed to have no significant local tension.

(4) The abdomen is filled with fluid which generates a hydrostatic gradient in pressure.

(5) The model mechanics of the diaphragm follow Laplace's law.

(6) The thorax is upright in a gravitational field.

(7) The pressure everywhere above the diaphragm is equal and is represented as Ppl.

Based on these assumptions, we can calculate the two principle radii of curvature of the mathematical model surface. In a three dimensional coordinate system, using the

Laplace law, the following mathematical model for the diaphragm was derived:

$$R''=2R+\frac{3(R')^2}{R'}-\frac{R'}{R^2}\cot(a)[R^2+(R')^2]-\frac{1}{T}\left[\frac{P0+\rho gH}{R}-\rho g\cos(a)\right]*[R^2+(R')^2]^{3/2}$$

This model indicates that there must be tension(T) for the diaphragm to have the dome shape. If T=0, then the radius of the curve R in Figure 1 approach infinity and the diaphragm is flat. The fluid in the abdomen tends to pull the dome of the diaphragm down and thus deforms it from the spherical shape it would have if tension and transdiaphragmatic pressure were the only contributing factors. The experiment of the model shows that the higher the density of the fluid in the abdomen is, the lower and narrower the dome surface is. It is the tension, transdiphragmatic pressure, and the hydrostatic gradient which draw the upper surface of the abdominal fluid into a curved dome or it will become a flat horizontal surface.

In figure A.16 to A.19, we found that P/Te is relatively independent of lung volume. When the lung volume changes, the shape of the diaphragm changes. This result partially explains why the length-tension characteristics outweigh geometric considerations in explaining diaphragm functions(2).

The simulated results comparing the diaphragms from two ascites patients with that of a normal patient's suggests that the two patients have higher transdiaphragmatic pressure comparing with the normal patient's.

One of the major causes of respiratory failure is the weakness of inspiratory muscles. It may occur in many clinical circumstance. The diaphragm is the most important inspiratory muscle. The establishment of this three dimensional simulated diaphragm model may help to quantify the shape, curvature and length of the diaphragm, which may make a contribution to the study of the function of the diaphragm.

# APPENDIX A

## DIAPHRAGM MODEL CURVES

This appendix include 22 figures of diaphragm model curves which are indicated in chapter 4.

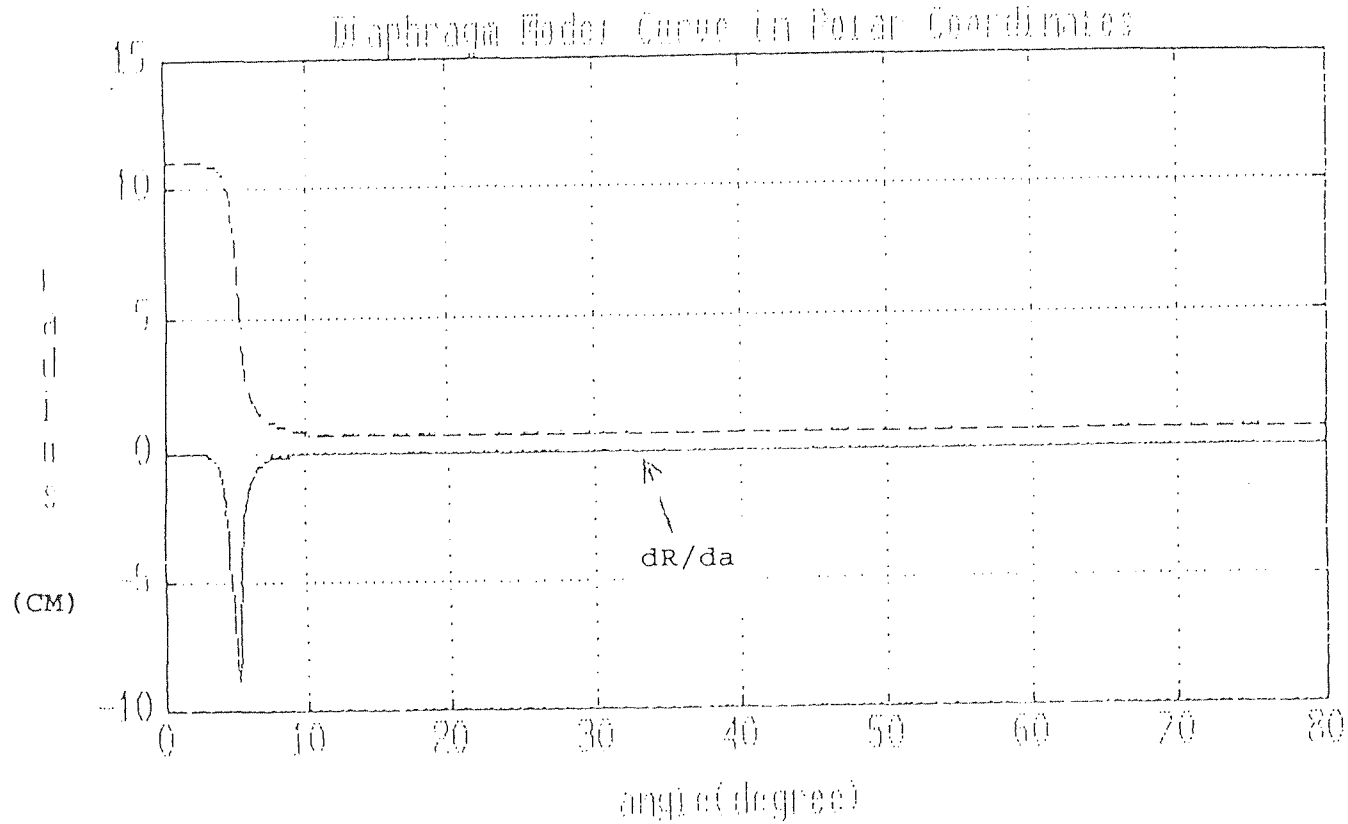


**Figure A.1** Diaphragm model curve in polar coordinates while r0=11cm, te=0.03N/cm.

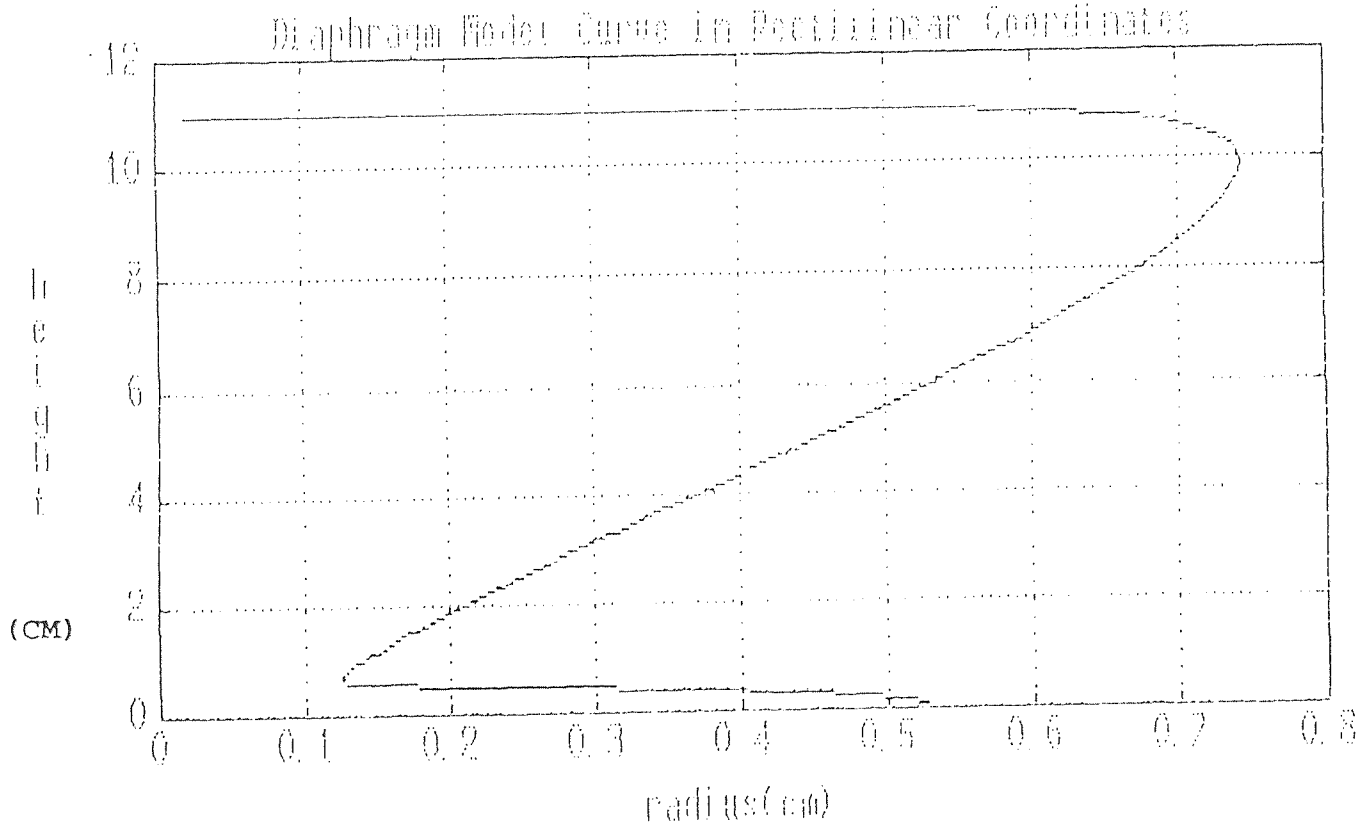


Figure A.2 Diaphragm model curve in rectilinear coordinates while r0=11cm, te=0.03N/cm.

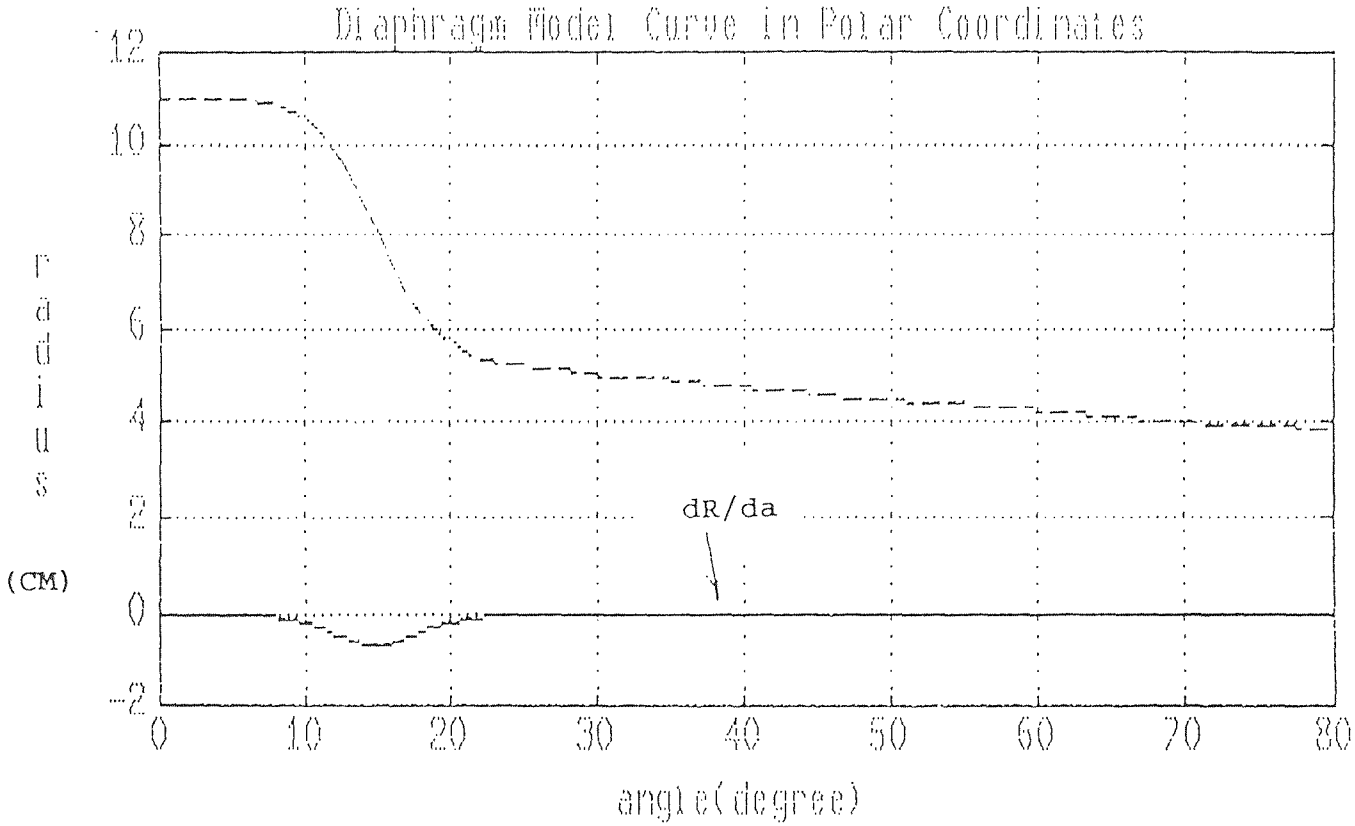


Figure A.3 Diaphragm model curve in polar coordinates while r0=11cm, te=0.3N/cm.

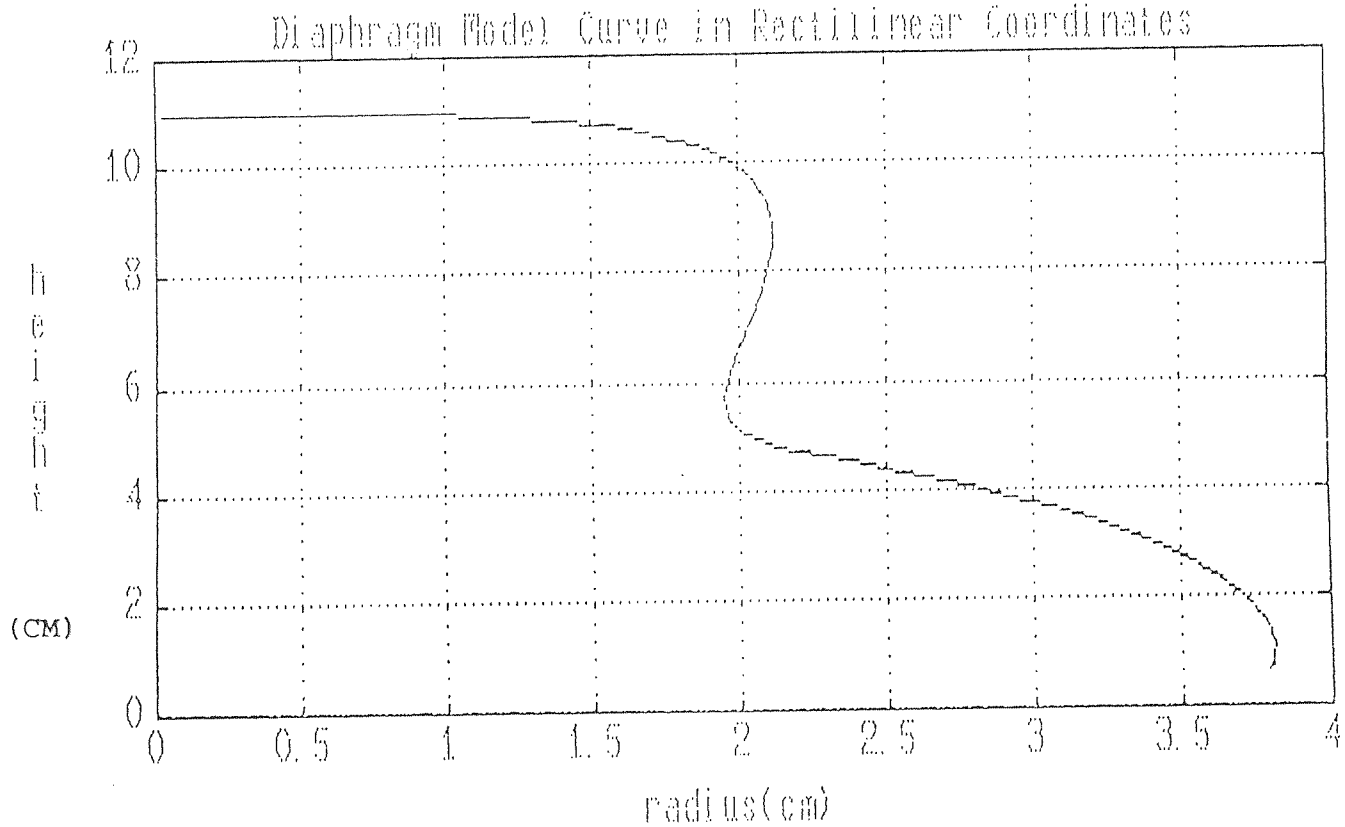


**Figure A.4** Diaphragm model curve in rectilinear coordinates while r0=11cm, te=0.3N/cm.

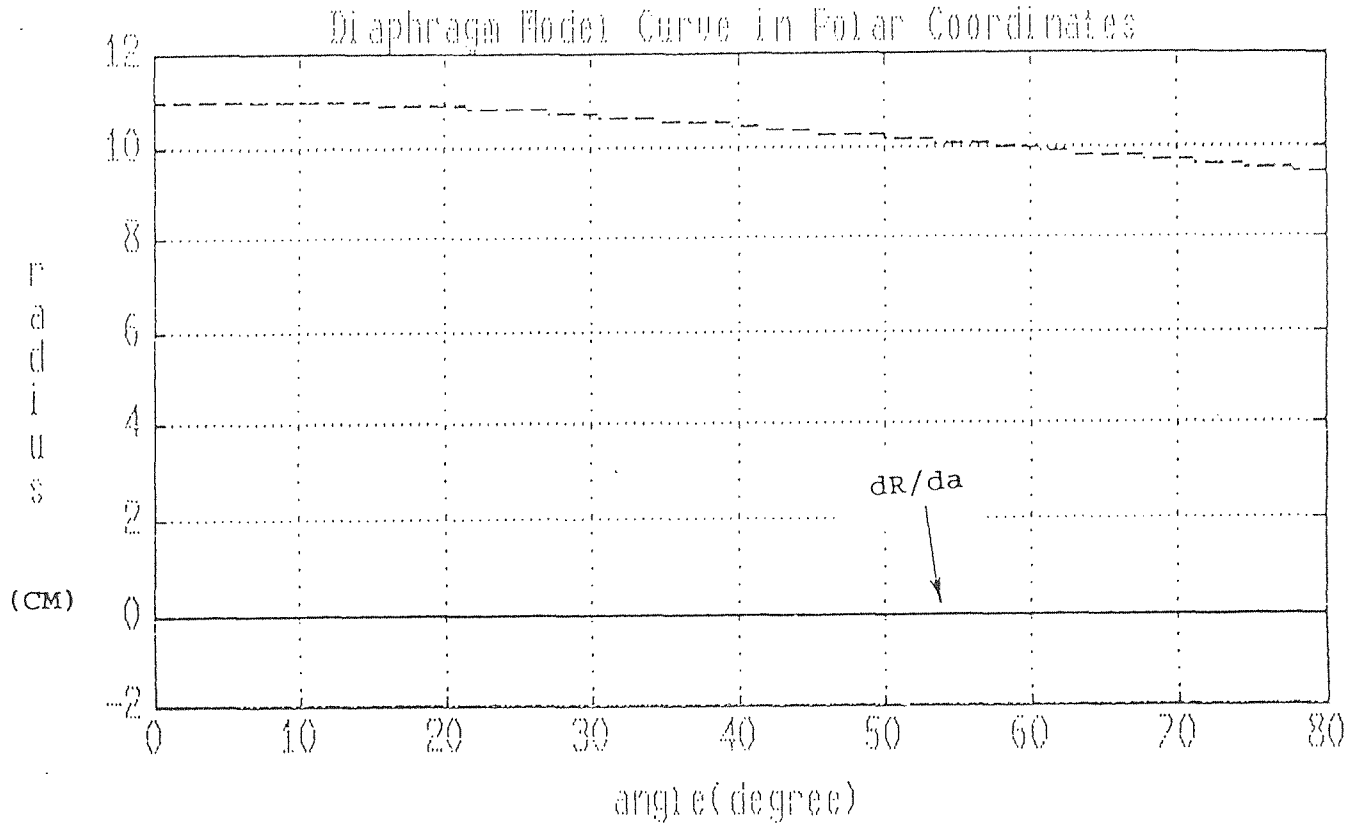


**Figure A.5** Diaphragm model curve in polar coordinates while r0=11cm, te=3N/cm.

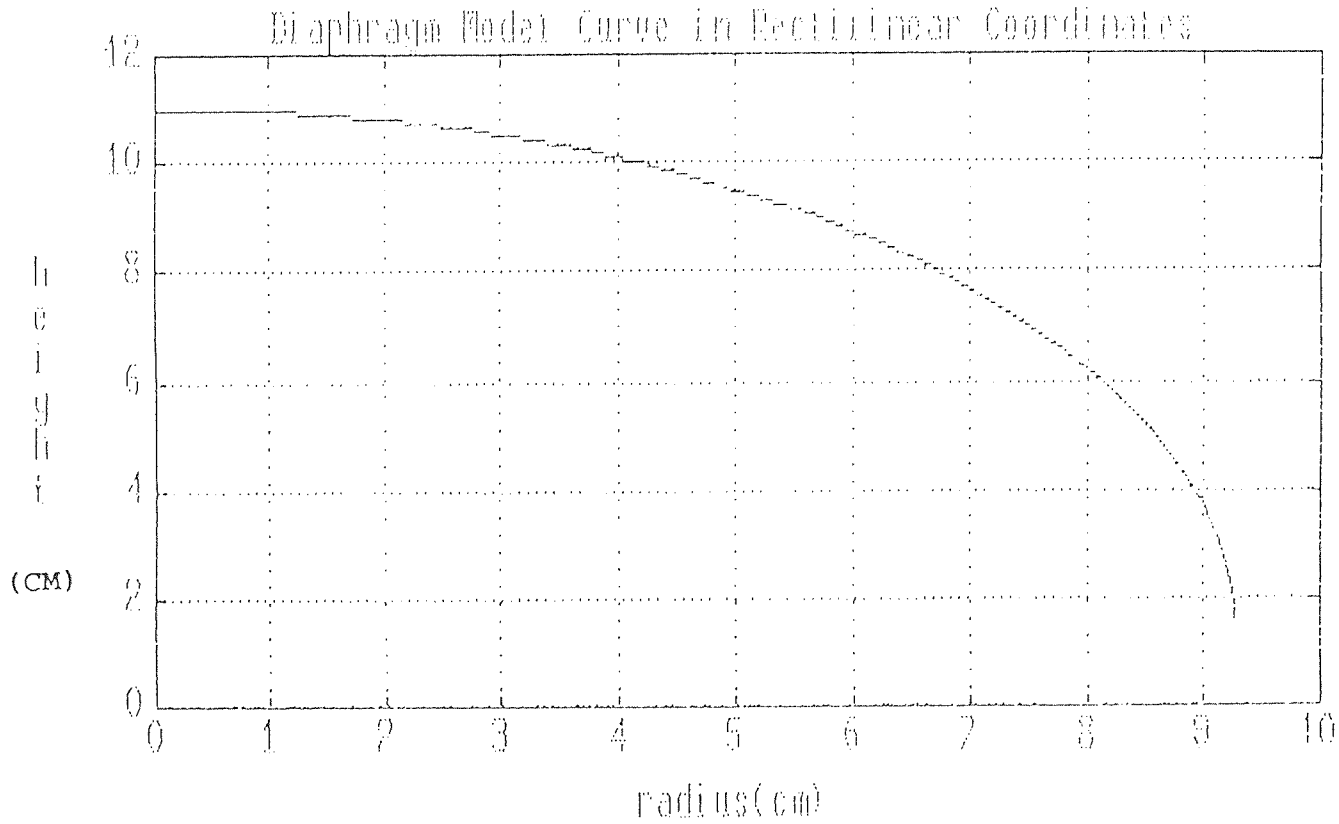


**Figure A.6** Diaphragm model curve in rectilinear coordinates while r0=11cm, te=3N/cm.

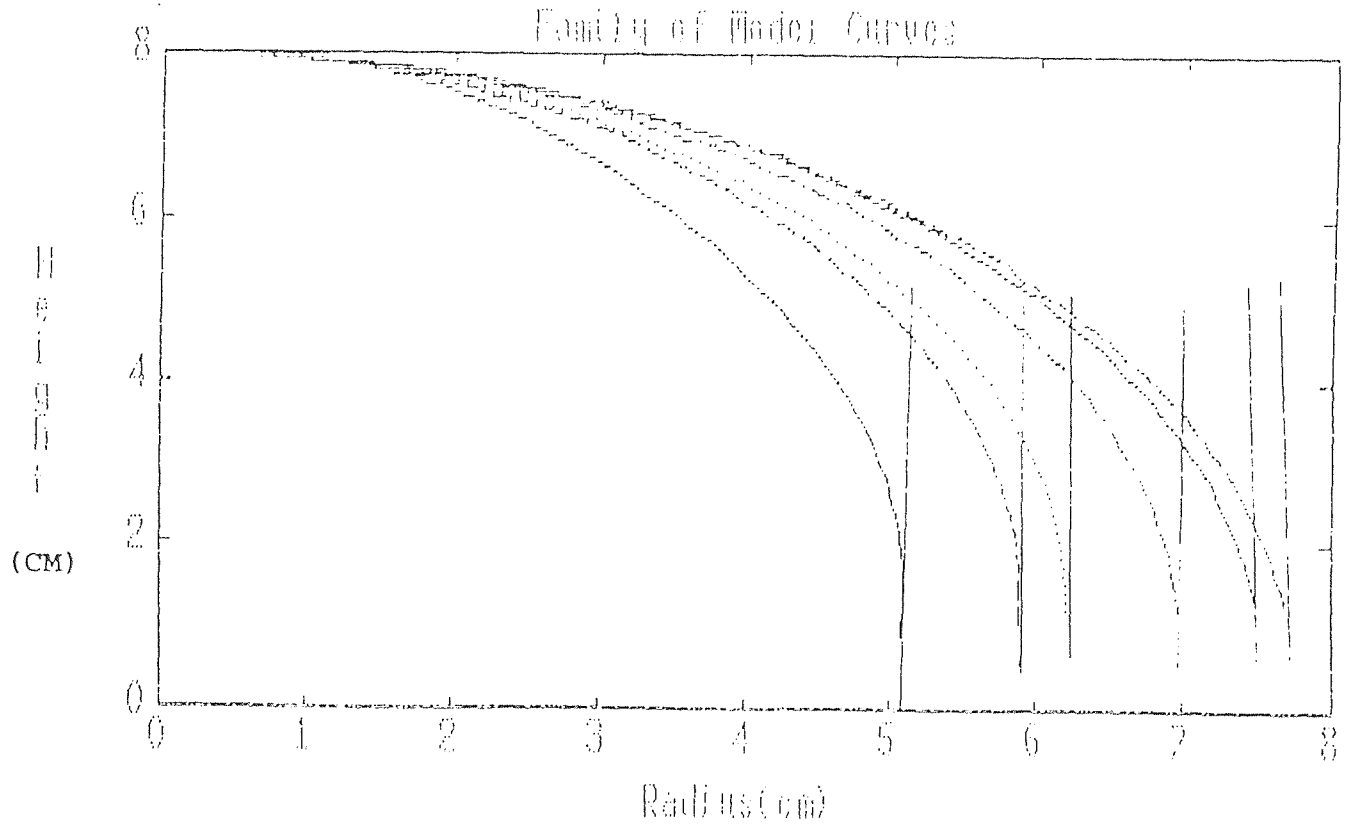


**Figure A.7** Family of solution to diaphragm model with different tensions, te= 0.5, 0.8, 1, 2, 5, 10N/cm (from left to right), and the same radius of curvature at the top of the dome equal to 8 cm. Vertical solid lines indicate the location of the rib cage.

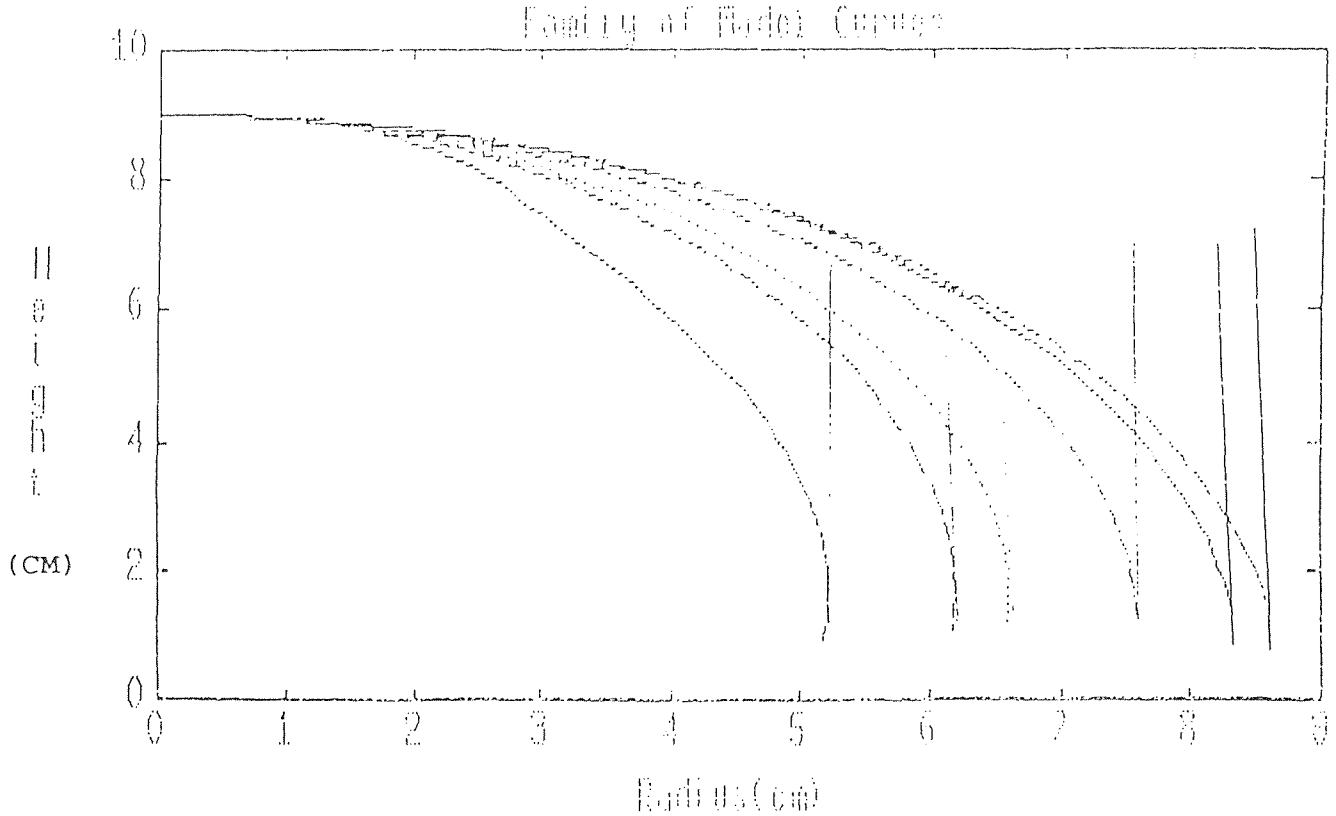


**Figure A.8** Family of solution to diaphragm model with different tensions, te= 0.5,0.8, 1, 2, 5, 10N/cm(from left to right), and the same radius of curvature at the top of the dome equal to 9 cm. Vertical solid lines indicate the location of the rib cage.

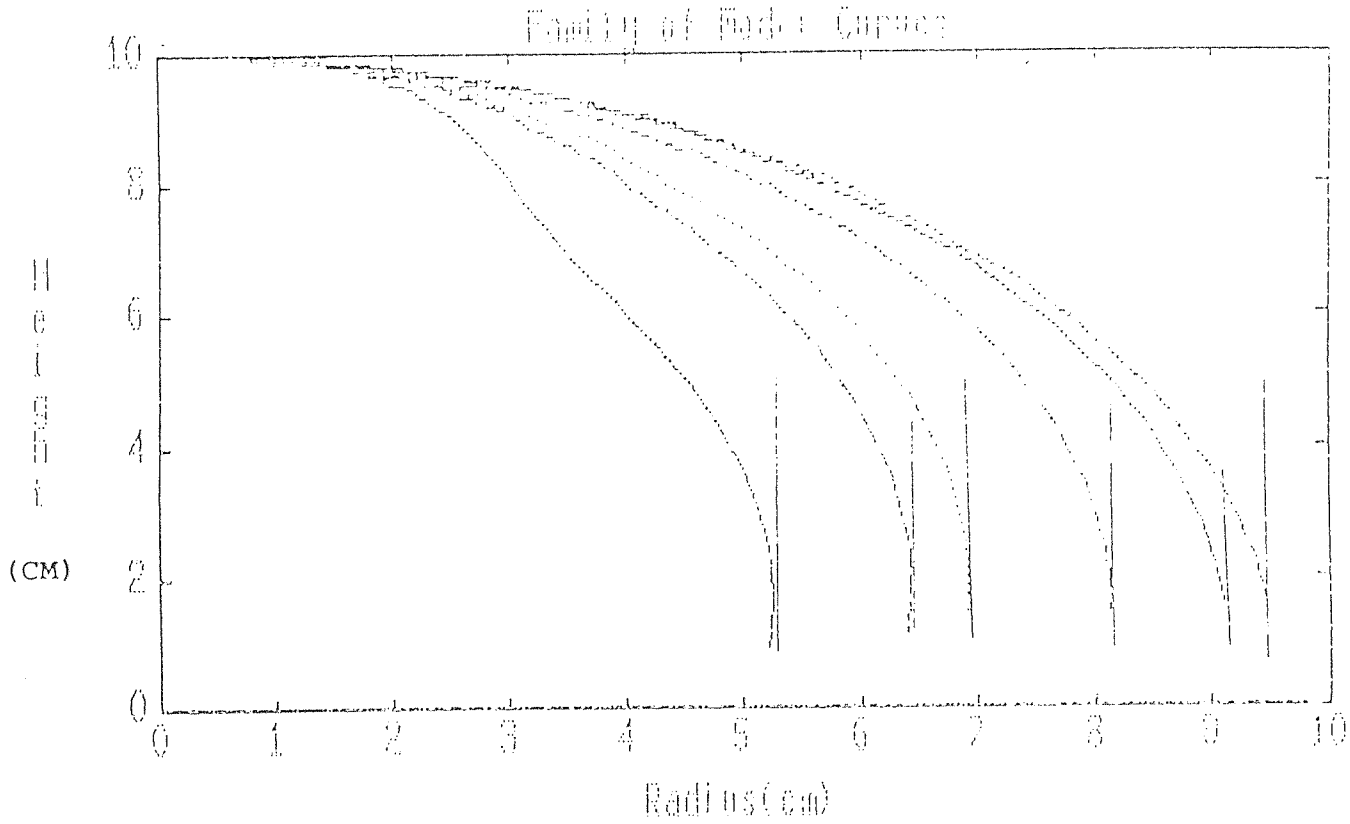


**Figure A.9** Family of solution to diaphragm model with different tensions, te= 0.5, 0.8, 1, 2, 5, 10N/cm (from left to right), and the same radius of curvature at the top of the dome equal to 10 cm. Vertical solid lines indicate the location of the rib cage .

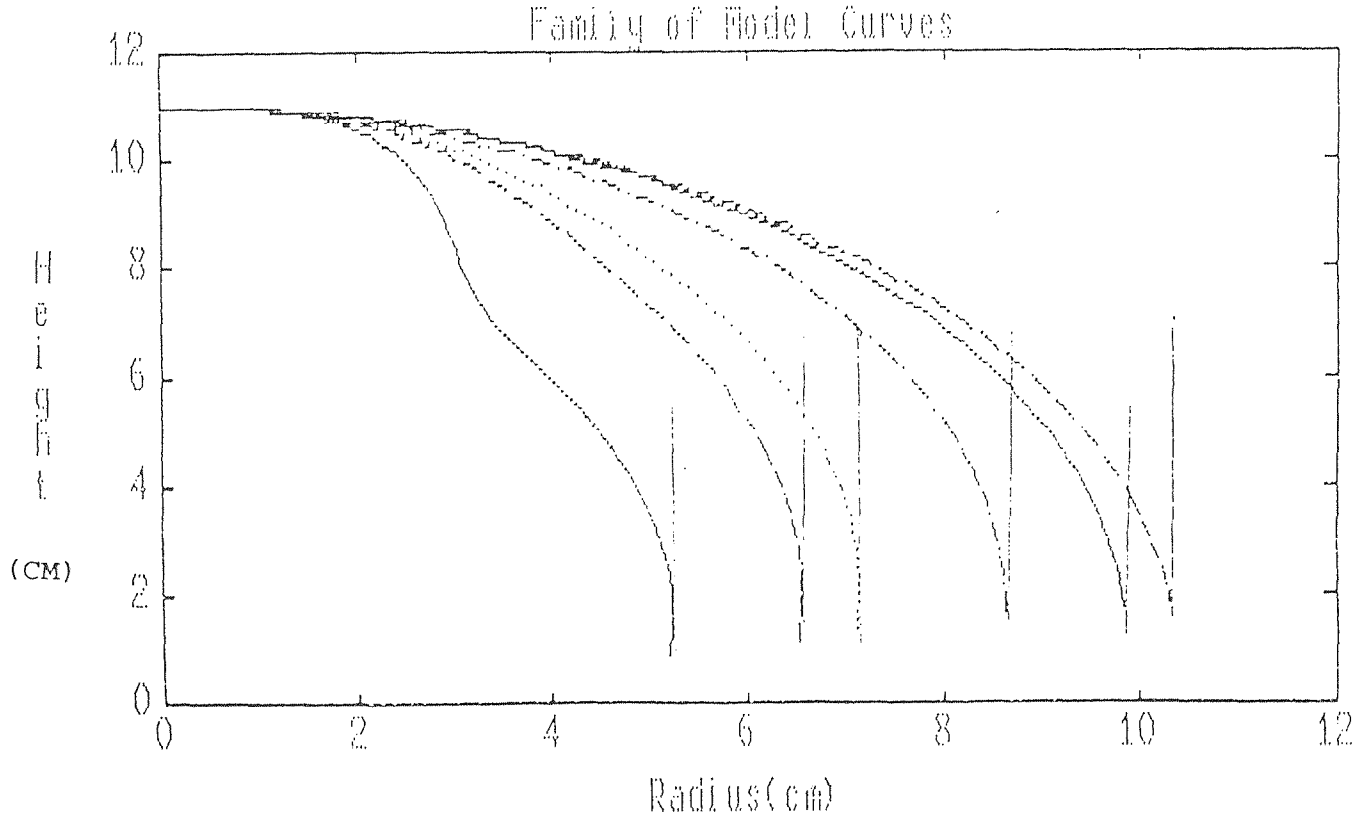


**Figure A.10** Family of solution to diaphragm model with different tensions, te= 0.5, 0.8, 1, 2, 5, 10N/cm (from left to right), and the same radius of curvature at the top of the dome equal to 11 cm. Vertical solid lines indicate the location of the rib cage .

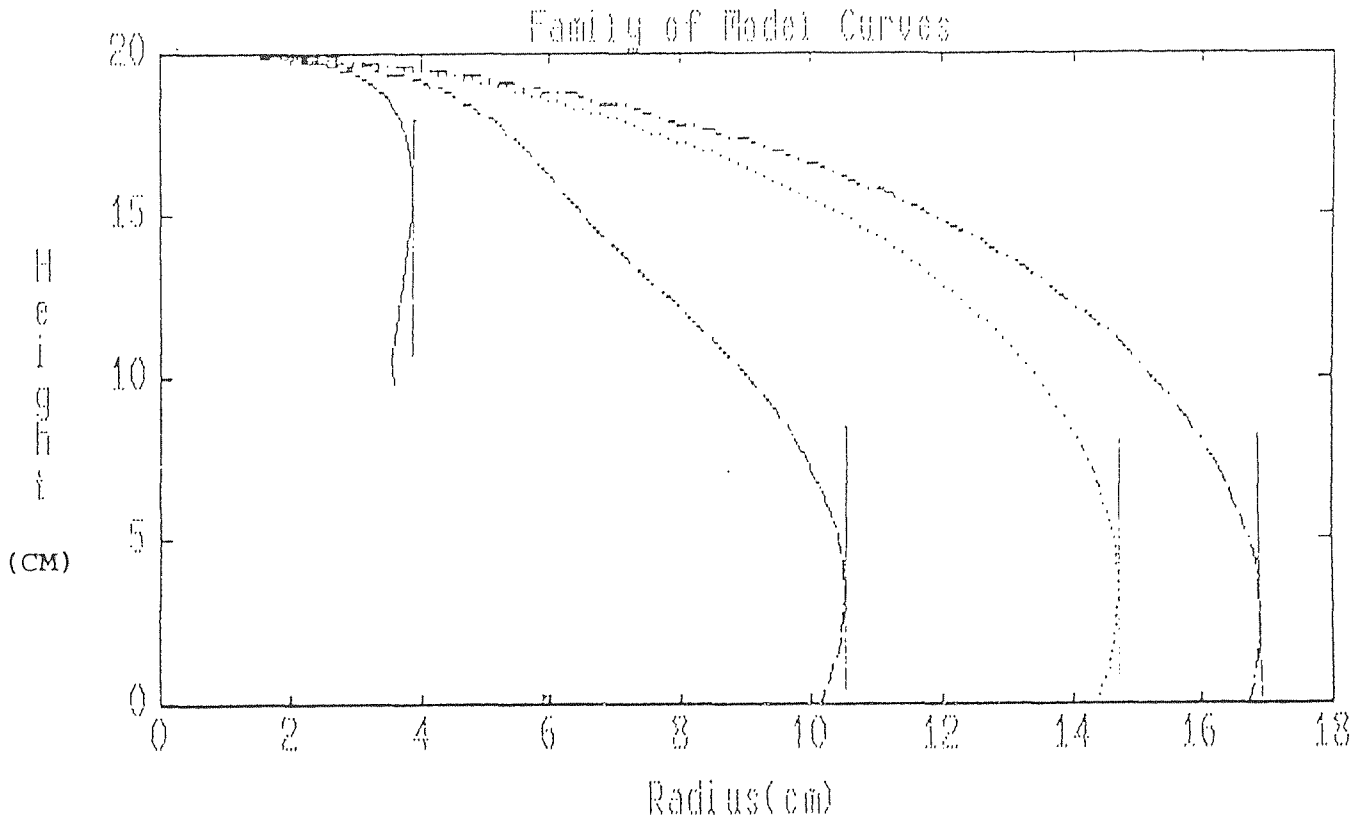


**Figure A.11** Family of solution to diaphragm model with different tensions, te=1, 2, 5, 10N/cm (from left to right), and the same radius of curvature at the top of the dome equal to 20 cm. Vertical solid lines indicate the rib cage sizes.

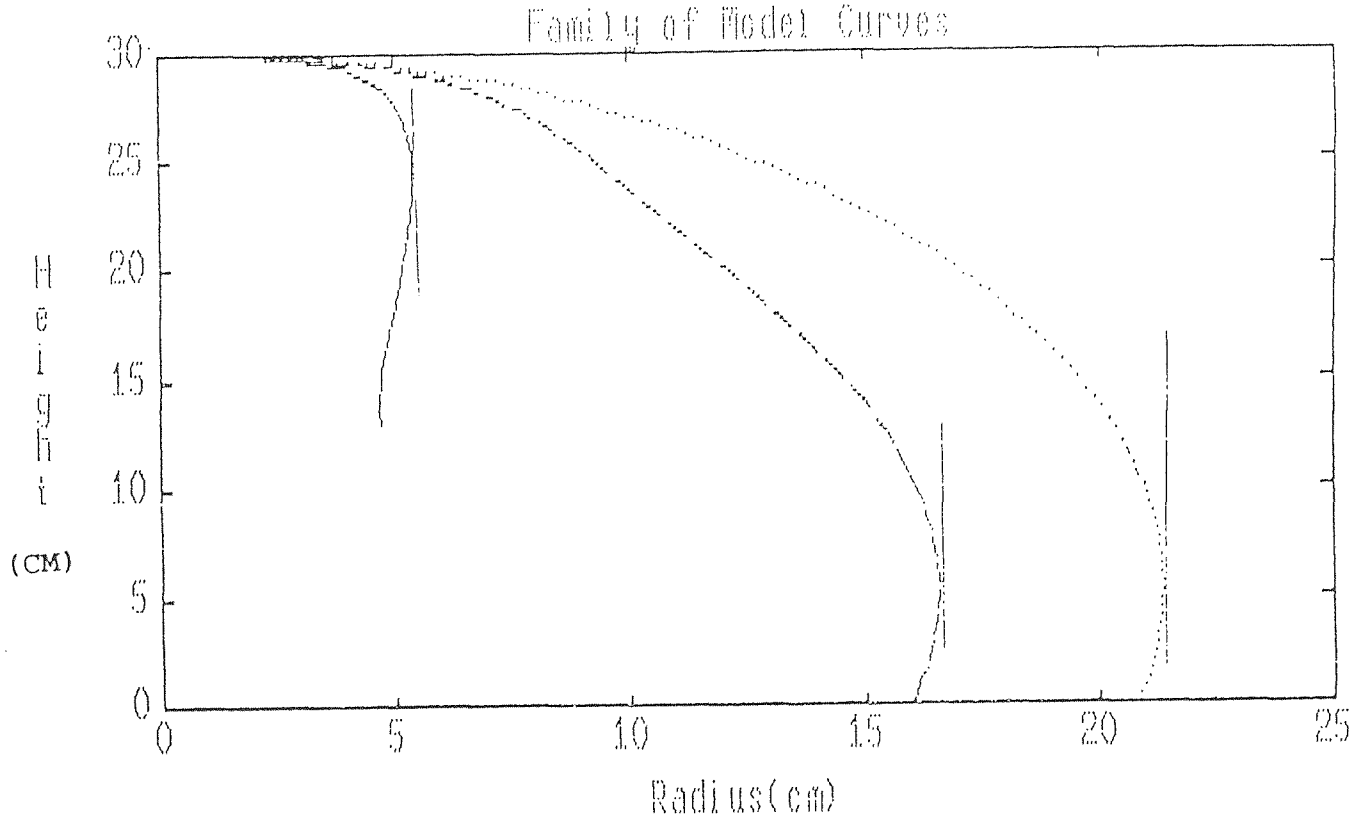


**Figure A.12** Family of solution to diaphragm model with different tensions, te= 5, 10N/cm (from left to right), and the same radius of curvature at the top of the dome equal to 30 cm. Vertical solid lines indicate the location of the rib cage.

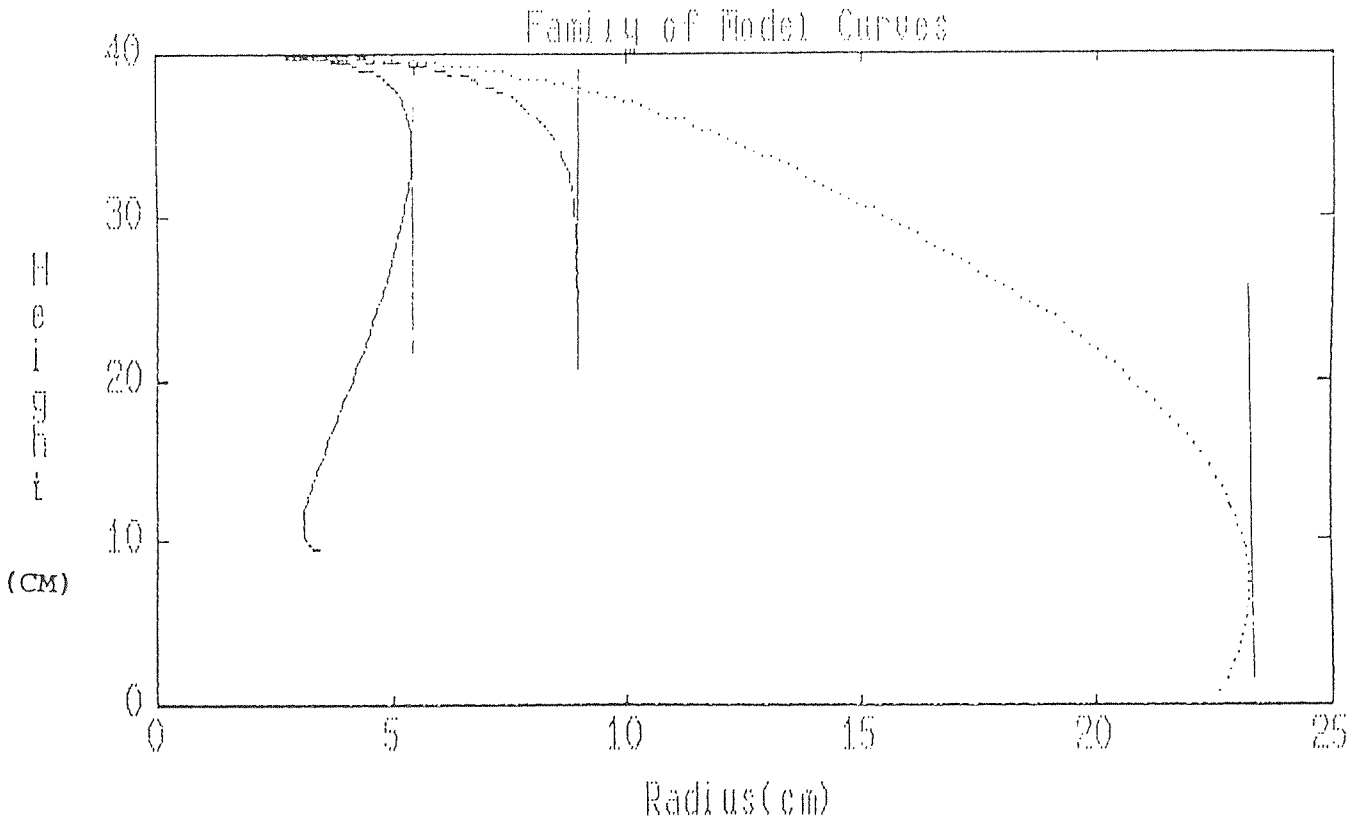


**Figure A.13** Family of solution to diaphragm model with different tensions, te=5, 10N/cm (from left to right), and the same radius of curvature at the top of the dome equal to 40 cm. Vertical solid lines indicate the location of the rib cage.

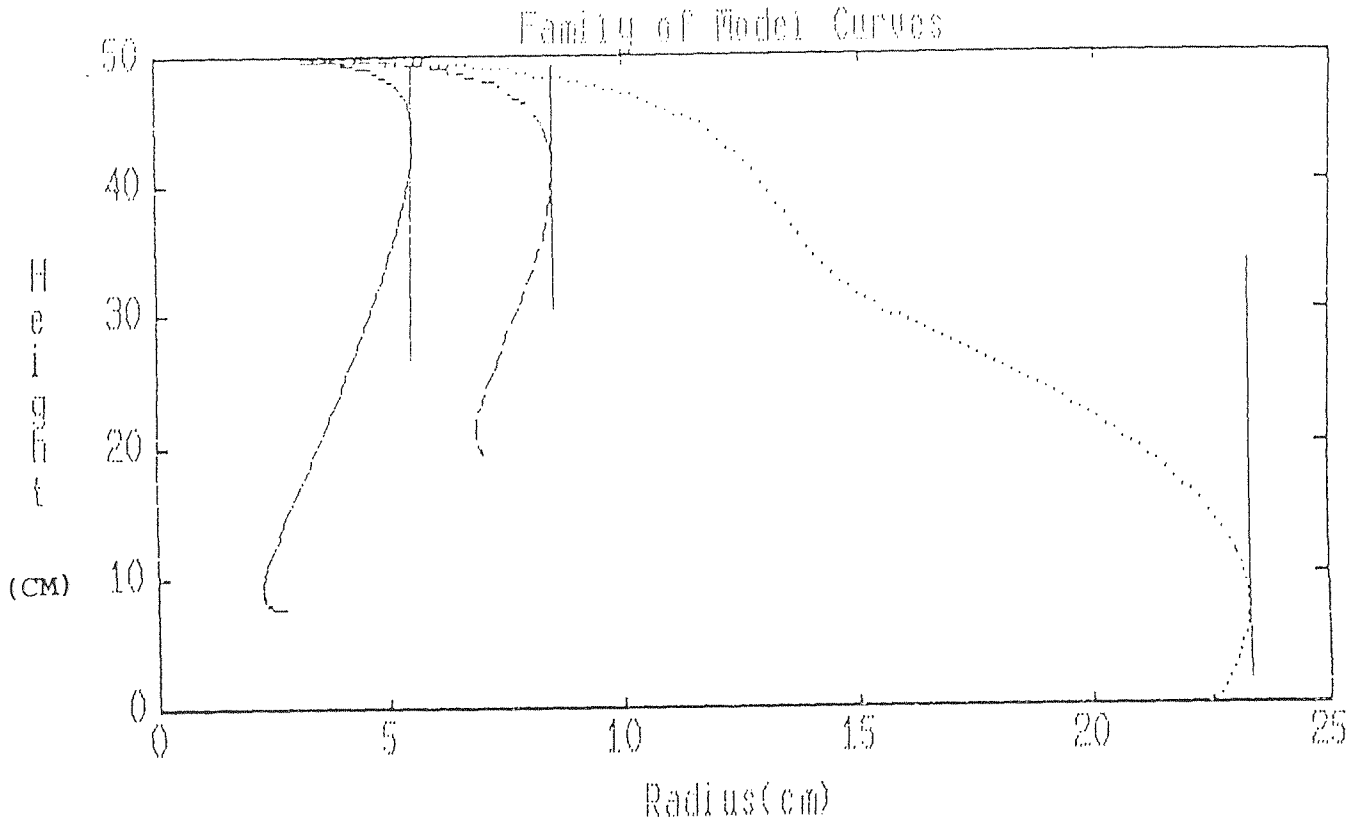


**Figure A.14** Family of solution to diaphragm model with different tensions, te=5, 10N/cm. (from left to right), and the same radius of curvature at the top of the dome equal to 50 cm. Vertical solid lines indicate the location of the rib cage.

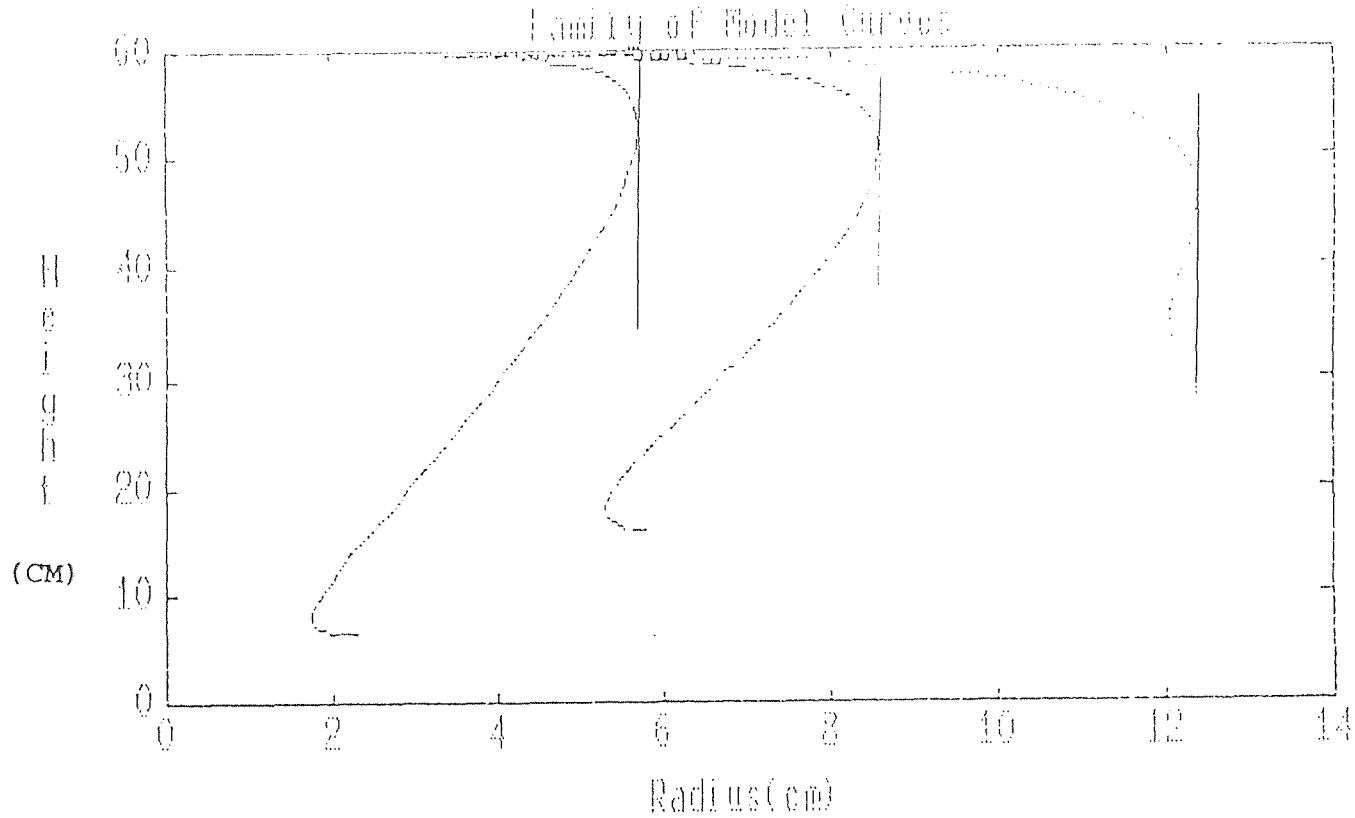


**Figure A.15** Family of solution to diaphragm model with different tensions, te= 5, 10N/cm (from left to right), and the same radius of curvature at the top of the dome equal to 60 cm. Vertical solid lines indicate the location of the rib cage.

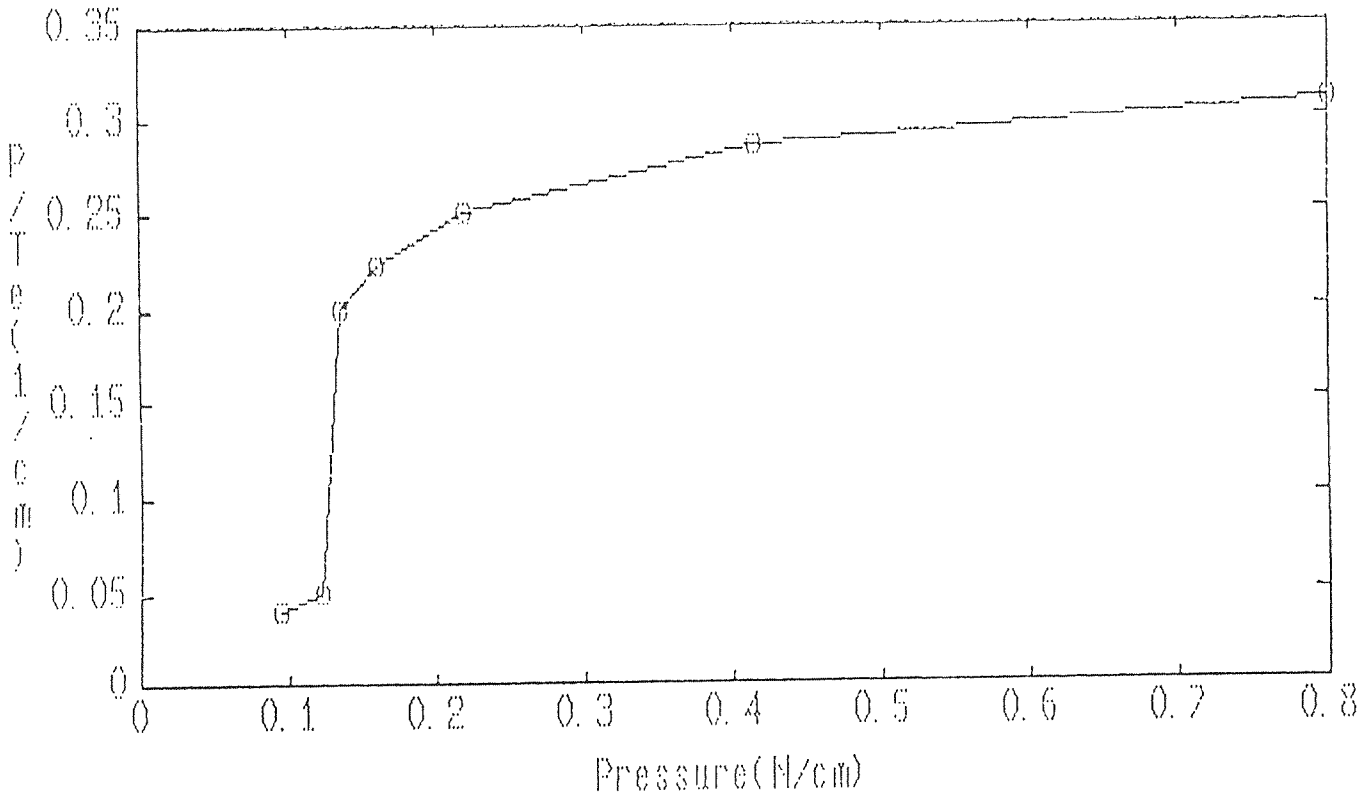


**Figure A.16** The ratio of transdiaphragmatic pressure to tension P/te against P, while rib cage radius equal to 6cm.

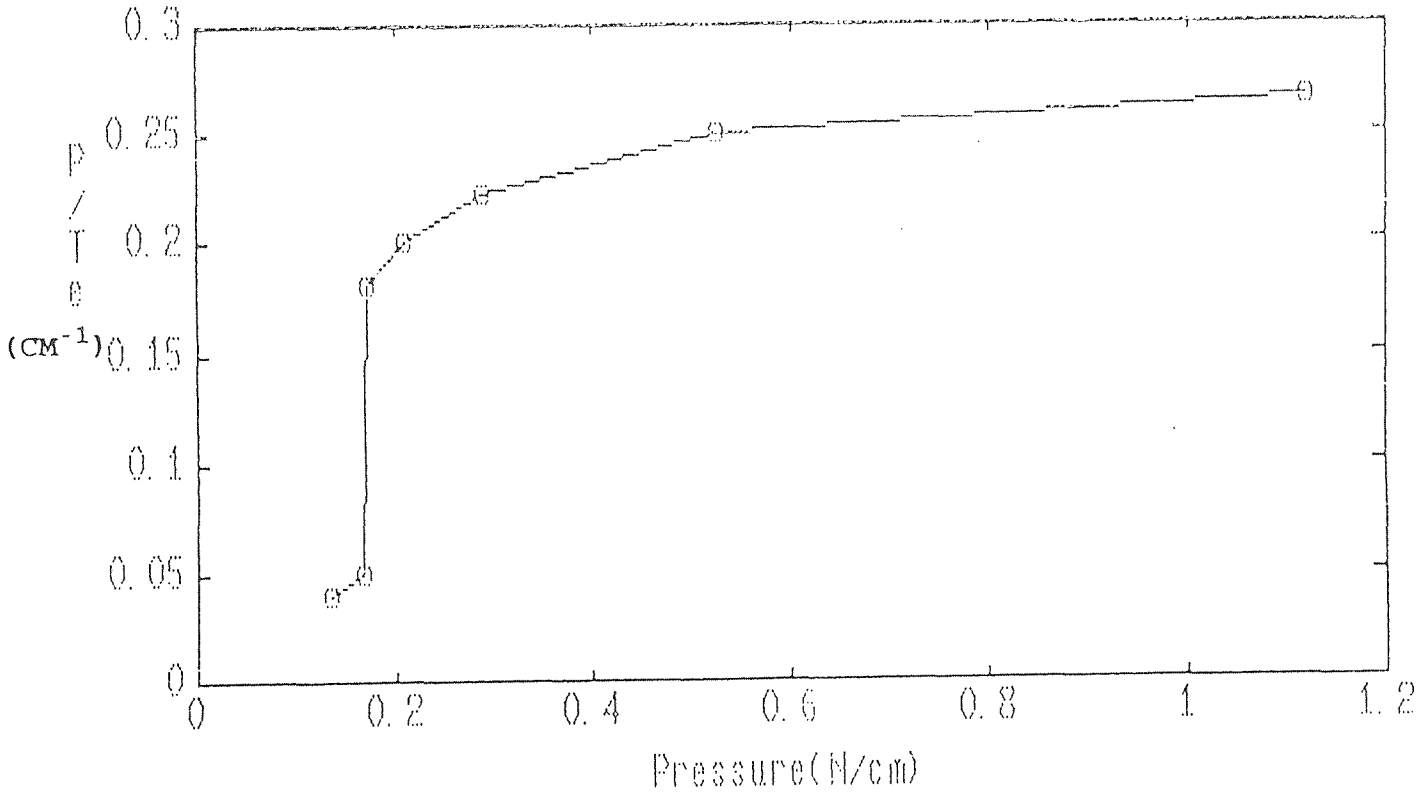


Figure A.17 The ratio of transdiaphragmatic pressure to tension P/te against P, while rib cage radius equal to 7cm.

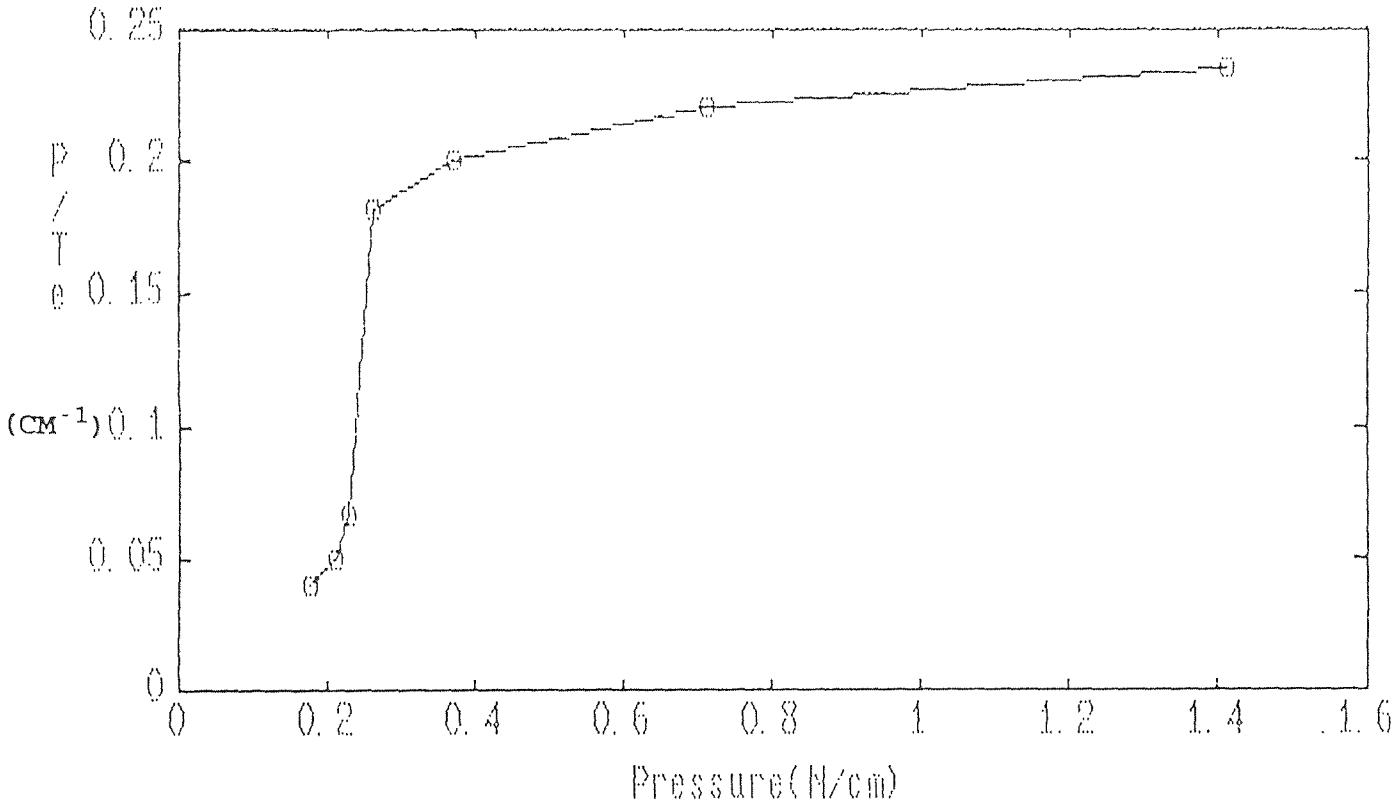


**Figure A.18** The ratio of transdiaphragmatic pressure to tension P/te against P, while rib cage radius equal to 8cm.

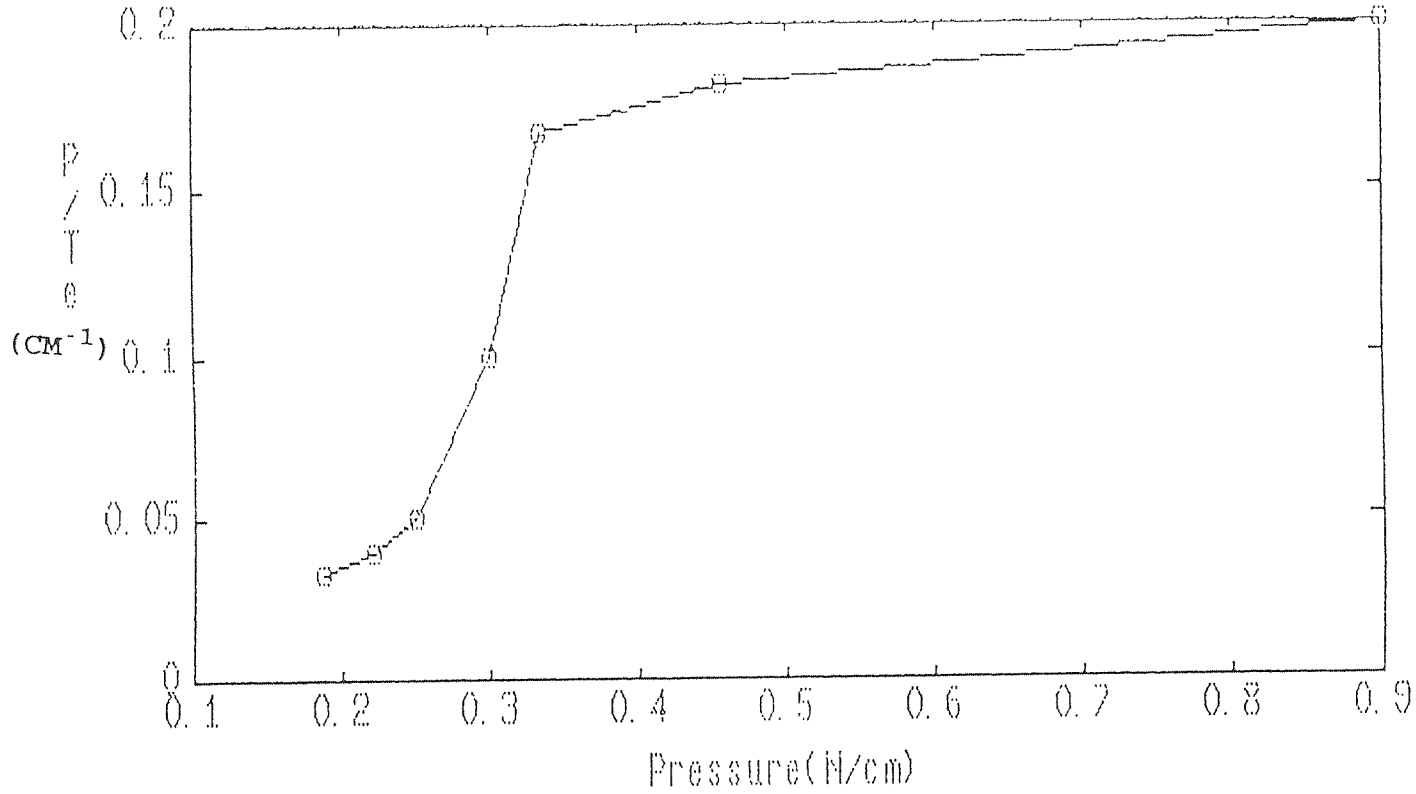


**Figure A.19** The ratio of transdiaphragmatic pressure to tension P/te against P, while rib cage radius equal to 9cm.

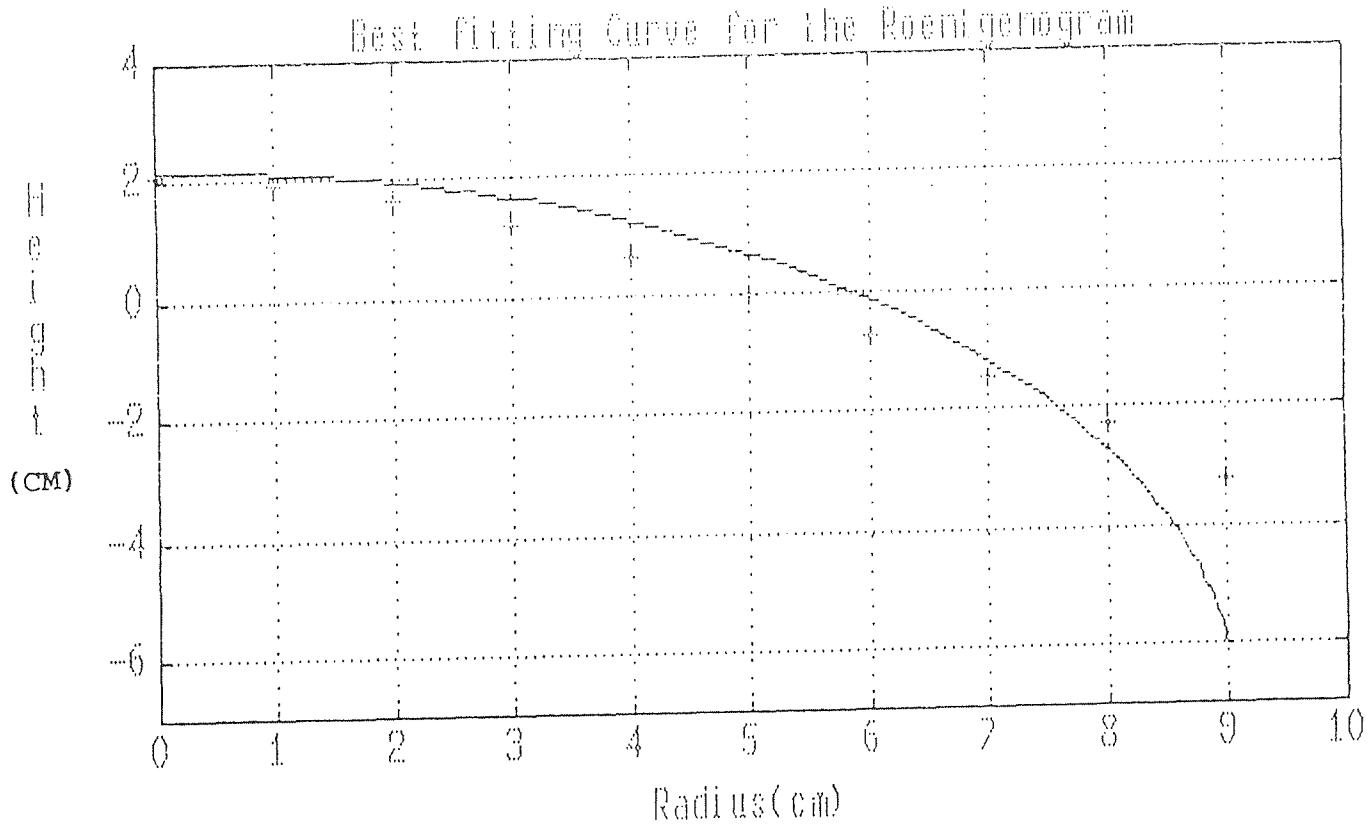


**Figure A.20** Best fitting curve for the diaphragm roentgenogram of ascites patient A, Te=4.5N/cm, P=0.9 $N/cm^2$.

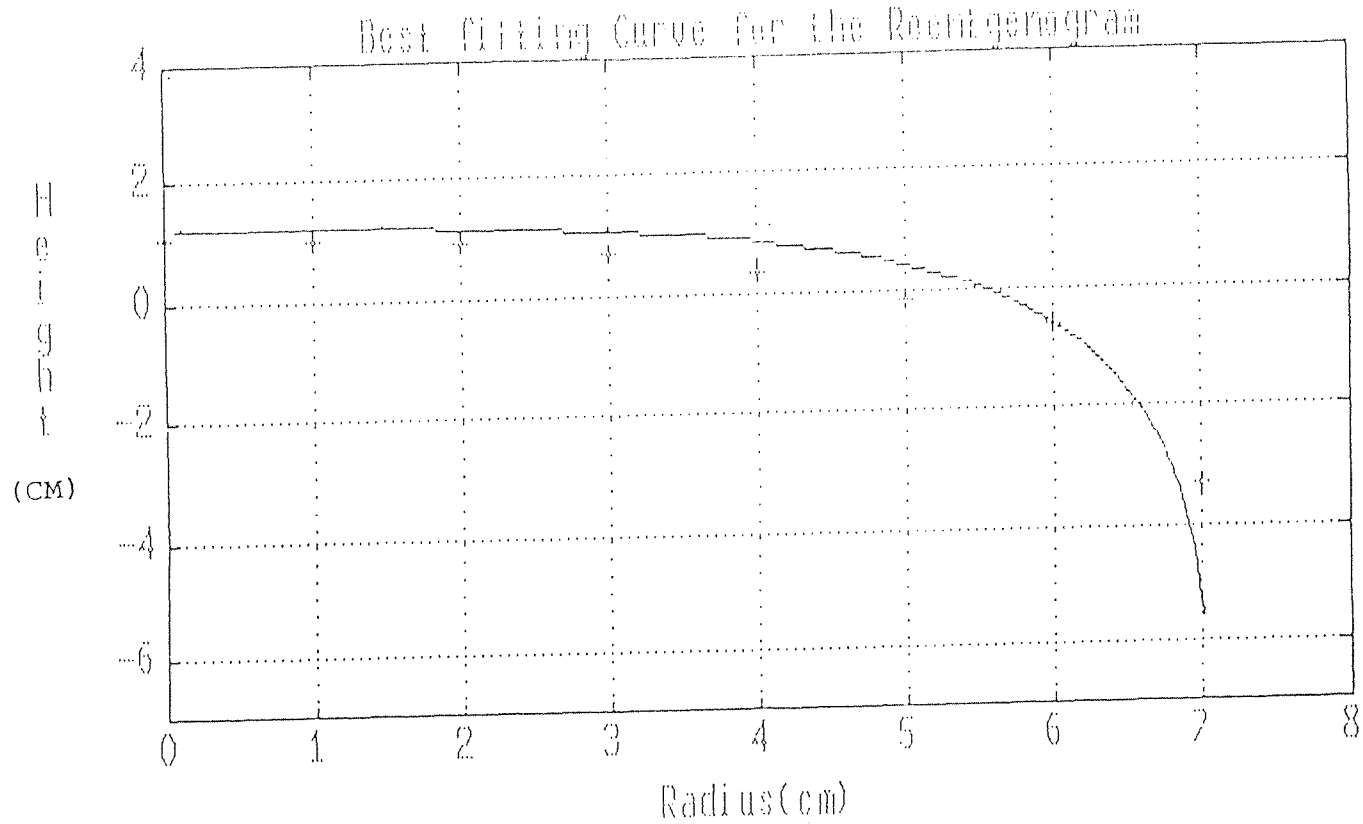


Figure A.22 Best fitting curve for the diaphragm roentgenogram of a normal person, Te=3.35N/cm, P=0.168N/cm$^2$.

# APPENDIX B

## DERIVATION OF RADII

### 1 THE DERIVATION OF r1

Suppose in a rectilinear system,the curve shown in Fig 1 be defined as x=x(t), y=y(t). t is the only parameter which can determine the value of x and y.

$$\tan w = \frac{dy}{dx} = \frac{dy/dt}{dx/dt} = \frac{y'}{x'}$$

Taking the derivate of both sides with respect to s, we have

$$\sec^2 w \frac{dw}{ds} = \left(\frac{y''}{x'} - \frac{x''y'}{x'^2}\right) * \frac{dt}{ds}$$

Because

$$\sec^2 w = 1+\tan^2 w = 1+\left(\frac{y'}{x'}\right)^2$$

and

$$\frac{dt}{ds} = \frac{dt}{\sqrt{dy^2+dx^2}} = \frac{1}{\sqrt{y'^2+x'^2}}$$

we obtain

$$\frac{dw}{ds} = \frac{1}{\sqrt{x'^2+y'^2}} * \frac{x'y''-y'x''}{x'^2} * \frac{1}{1+(y'/x')^2}$$

$$= \frac{x'y''-y'x''}{\sqrt{x'^2+y'^2}} \qquad (18)$$

Let's transfer the result from rectiliner coordinates to polar coordinates, and let t=a( because angle a is the parameter which can independantly determine the x and y).

Let

$R=R(a)$; $R'=dR(a)/da$; $R''=d^2R(a)/d^2a$;

$x=R*\cos(a)$;

$y=R*\sin(a)$;

We have

$x'=R'*\cos(a)-R*\sin(a)$;

$y'=R'*\sin(a)+R*\cos(a)$;

$x''=R''*\cos(a)-2*R'*\sin(a)-R*\cos(a)$;

$y''=R''*\sin(a)+2*R'*\cos(a)-R*\sin(a)$;

Also we have

$$x'^2+y'^2$$

$$= [R'*\cos(a)-R*\sin(a)]^2+[R'*\sin(a)+R*\cos(a)]^2$$

$$= R'^2*\cos^2(a)-2*R*R'*\sin(a)*\cos(a)+R^2*\sin^2(a)$$

$$+R'^2*\sin^2(a)+2*R*R'\sin(a)*\cos(a)+R^2*\cos^2(a)$$

$$=R'^2+R^2$$

and

$$x'y''-y'x''$$

$$=(R'*\cos(a)-R*\sin(a))*(R''*\sin(a)+2*R'*\cos(a)-R*\sin(a))$$

$$-(R'*\sin(a)+R*\cos(a))*(R'*\cos(a)-2*R'*\sin(a)-R*\cos(a))$$

$$=R'R''\sin(a)\cos(a)+2(R')^2\cos^2(a)-RR'\sin(a)\cos(a)$$

$$-RR'\sin^2(a)-2RR'\sin(a)\cos(a)+R^2\sin^2(a)$$

$$-R'R''\sin(a)\cos(a)+2(R')*2\sin^2(a)+RR'\sin(a)\cos(a)$$

$$-RR''\cos^2(a)+2RR'\sin(a)\cos(a)+R^2\cos^2(a)$$

$$=2(R')^2-RR''+R^2$$

So that

$$\frac{dw}{ds} = \frac{2(R')^2-RR''+R^2}{[(R')^2+R2]^{3/2}}$$

$$r1=(dw/ds)^{-1} = \frac{[(R')^2+R^2]^{3/2}}{2(R')^2-RR''+R^2} \qquad (19)$$

## 2 THE DERIVATION OF r2

From Figure 2, we can get

$R=R(a)$

$x=R(a)\sin(a)\cos(b)$

$y=R(a)\sin(a)\sin(b)$

$z=R(a)\cos(b)$

In these equations, x, y, z, and R are dependent variables, a and b are independent variables. We can obtain the partial derivatives of x, y, z

$x_a=R'(a)\sin(a)\cos(b)+R(a)\cos(a)\cos(b)$

$x_b=-R(a)\sin(a)\sin(b)$

$x_{aa}=[R''\sin(a)+2R'\cos(a)-R\sin(a)]\cos(b)$

$x_{bb}==-R\sin(a)\cos(b)$

$x_{ab}=-\sin(b)[R'(a)\sin(a)+R\cos(a)]$

$y_a=[R'\sin(a)+R\cos(a)]\sin(b)$

$y_b=R(a)\sin(a)\cos(b)$

$y_{aa}=[R''\sin(a)+2R'\cos(a)-R\sin(a)]\sin(b)$

$y_{bb}=-R\sin(a)\sin(b)$

$y_{ab}=[R'\sin(a)+R(a)\cos(a)]\cos(b)$

$z_a=R'\cos(a)-R\sin(a)$

$z_b=0$

$z_{aa}=R''\cos(a)-2R'\sin(a)-R\cos(a)$

$z_{bb}=0$

$z_{ab}=0$

Substituing these partial derivatives to former formulas (4) to (14) , we have

$$E=x_a^2+y_a^2+z_a^2$$
$$=[R'\sin(a)+R\cos(a)]^2+[R'\cos(a)-R\sin(a)]^2+0$$
$$=R^2+(R')^2$$

$$F=x_a x_b+y_a y_b+z_a z_b$$
$$=[R'\sin(a)+R\cos(a)]\cos(b)[-R\sin(a)\sin(b)]$$
$$+[R'\sin(a)+R\cos(a)]\sin(b)R\sin(a)\cos(b)+0$$
$$=0$$

$$G=x_b^2+y_b^2+z_b^2$$
$$=R^2\sin^2(a)$$

$$H = EG-F^2$$
$$=R\sin(a)[R^2+(R')^2]$$

$$E = \begin{vmatrix} x_{aa} & y_{aa} & z_{aa} \\ x_a & y_a & z_a \\ x_{ab} & y_{ab} & z_{ab} \end{vmatrix}$$

$$=x_{aa}y_a z_{ab}+x_a y_{ab} z_{aa}+x_{ab} z_a y_{aa}$$
$$-x_{ab}y_a z_{aa}-x_{aa}y_{ab} z_a-x_a y_{aa} z_{ab}$$
$$=0+R\sin(a)\cos^2(b)[R'\sin(a)+R\cos(a)]$$
$$*[R''\cos(a)-2R'\sin(a)-R\cos(a)]$$
$$-R\sin(a)\sin^2(b)[R''\sin(a)+2R'\cos(a)-R\sin(a)]$$
$$*[R'\cos(a)-R\sin(a)]+R\sin(a)\mathrm{sib}^2(b)$$
$$*[R'\sin(a)+R\cos(a)][R''\cos(a)-2R'\sin(a)-R\cos(a)]$$
$$-R\sin(a)\cos^2(b)[R'\cos(a)-R\sin(a)]$$
$$*[R''\sin(a)+2R'\cos(a)-R\sin(a)]-0$$
$$=[R\sin(a)\cos^2(b)+R\sin(a)\sin^2(a)]$$
$$*[(R'\sin(a)+R\cos(a))(R''\cos(a)-2R'\sin(a)-R\cos(a))$$
$$-(R''\sin(a)+2R'\cos(a)-R\sin(a))(R'\cos(a)-R\sin(a))]$$
$$=R\sin(a)[-2(R')^2+RR''-R^2]$$

$$F' = \begin{vmatrix} x_{ab} & y_{ab} & z_{ab} \\ x_a & y_a & z_a \\ x_b & y_b & z_b \end{vmatrix}$$

Because $z_{ab}=zb=0$, So that

$$F'=x_b y_{ab} z_a-x_{ab} y_b z_a$$
$$=R\sin(a)[R'\cos(a)-R\sin(a)]$$
$$*[\cos(b)(-\sin(b)-(-\sin(b))\cos(b)]$$
$$=0$$

$$G' = \begin{vmatrix} x_{bb} & y_{bb} & z_{bb} \\ x_a & y_a & z_a \\ x_b & y_b & z_b \end{vmatrix}$$

Because $z_{bb}=z_b=0$, so that

$$G' = (x_b y_{bb} - x_{bb} y_b) z_a$$

$$= R^2 \sin^2(a)[(-\sin(b))(-\sin(b)) - (-\cos(b))\cos(b)]$$

$$*[R'\cos(a) - R\sin(a)]$$

$$= R^2 \sin^2(a)[R'\cos(a) - R\sin(a)]$$

Substituting these parameters to equation

$$Ar^2 + Br + C = 0$$

We have

$$A = E'G' - F'^2$$

$$= R^3 \sin^3(a)[-2(R')^2 + RR'' - R^2] * [R'\cos(a) - R\sin(a)]$$

$$B = -H(G'E + GE' - 2FF')$$

$$C = H^4 = R^4 \sin^4(a)[(R')^2 + R^2]^2$$

$$\frac{C}{A} = \frac{R^4 \sin^4(a)[(R')^2 + R^2]^2}{R^3 \sin^3(a)[-2(R')^2 + RR'' - R^2] * [R'\cos(a) - R\sin(a)]}$$

$$= \frac{R\sin(a)[(R')^2 + R^2]^2}{[R^2 - RR'' + 2(R')^2] * [R\sin(a) - R'\cos(a)]}$$

$$= r1r2$$

$$= \frac{[(R')^2 + R^2]^{3/2}}{2(R')^2 - RR'' + R^2} * r2$$

So that

$$r2 = \frac{R\sin(a)[(R')^2 + R^2]^{1/2}}{R\sin(a) - R'\cos(a)} \qquad (20)$$

$$= \frac{[(R')^2 + R^2]^{1/2}}{1 - (R'/R)\cot(a)}$$

## APPENDIX C

## M-FILE BB.M

```
x0=[x1d r0]';
    % define the initial conditions, where x1d=x'(t0)
    % r0=radius when the angle equal to zero.

global r0
global ru
global te
    % make r0, ru, and te available in every M-file

[t,x]=ode23('hbu', t0, tf, x0);
    % Integrating the diaphragm equation. where t0, tf, and
    % x0 are initial conditions. t0 and tf represent the
    % start and the final angles, x0(1)=x'(t0), x0(2)=x(t0)

x1=x(:,2).*sin(t*pi/180.0);
y1=x(:,2).*cos(t*pi/180.0);
    % transfer the results from polar coordinate system
    % to rectilinear coordinate.

plot(t,x);
title('Diaphragm Simulate Curve in Polar Coordinates')
xlable('angle(degree)')
ylable('curvature radius(cm)')
```

```
grid
pause
    % plot the simulation curve in polar coordinate system

plot(x1,y1);
pause
    % plot the simulation curve in rectilinear coordinate
    % system. name and label the diagram.
```

## APPENDIX D

## M-FILE ZH.M

```
dn=max(size(d));
    % decide the size of the X-ray data
x1n=max(size(x1));
    % Obtain the size of the simulate curve data
dmax=max((max(d)));
    % dmax is the largest value of X-ray data in x
    %dimension

    % Cut the size of simulate curve in x dimension to the
    % same as the X-ray data's
for i=1:x1n
      a=x1(i);
      if a==dmax
        x2n=i;
        clear a
        break
      end
      if a>dmax
        x2n=i;
        a=y1(i)-y1(i-1))*(dmax-x1(i-1));
        b=x1(i)-x1(i-1);
        y1(i)=a/b+y1(i-1);
        clear a b
```

```
      end
 end
 pause

    % x2 and y2 are the simulate curve with the same x
    % dimension width as the X-ray data's
 for i=1:x2n
      x2(i)=x1(i);
      y2(i)=y1(i);
 end

    %Calculate the length of the diaphragm and the area
    %under the diaphragm
length=0;
area=0;

for i=2:x2n
    length=((x2(i)-x2(i-1))^2+(y2(i)-y2(i-1))^2)^0.5+length;
end

b=y2(x2n);

for i=1:x2n
    x21(i)=x2(i);
    y21(i)=y2(i)-b;
end
```

```
for i=2:x2n
    area=area+y21(i)*(x21(i)-x21(i-1));
end

    % transpose the matrixes from rows to columns.
x2=x2';
y2=y2';
pause

    % Chose the y value that its corresponding x value is
    % the same as the X-rays to make the results comparable
    % x3, y3 are the results
x3(1)=0;
y3(1)=y2(1);

for i=2:dn
      for j=2:x2n
        if x2(j)==d(i,1)
           x3(i)=x2(j);
           y3(i)=y2(j);
           break
        end
        if x2(j)>d(i,1)
           a=(y2(j)-y2(j-1))*(d(i,1)-x2(j-1));
           b=x2(j)-x2(j-1)
           y3(i)=a/b+y2(j-1);
           x3(i)=d(i,1);
```

```
            clear a b
          end
        end
end

     %transpose the matrixes from rows to columns
x3=x3'
y3=y3'
pause

     % make the y3 lower to the same level as the data
     % of X-ray film
y3mean=mean(y3)
pause

y3=y3-y3mean;
pause

     % y4 is the difference of the simulate curve data
     % and the X-ray data
y4=y3-d(:,2);

y4     % display y4
pause

n=max(size(y4));
```

```
sf=sum(y4.^2)/n; % sf  is the square  difference.
                 % The less it is, the better the curve
                 % fit is.
pause

     %display the results
sf
r0
length
area
pause

     % plot the x-ray data and the simulation cur
     % at the same diagram. name and label it.
plot(x2, y2-y3mean, d(:,1), d(:,2),'+');
title('Best fitting curve for the Roentgenogram')
xlabel('Radius(cm)')
ylabel('Height(cm)')
grid
pause
pause
clear x2 x3 y2 y3 y4 sf
```

## REFERENCES


1. Agostoni, E. P., P. Mognoni, and J. Mead. 1965. "Relation Between Changes of Rib Cage Circumference and Lung Volume." *J. Appl. Physiol.* 20:1179-1186.

2. Kim, M. J., W. S. Druz, J. Danon, W. Machnach, and J. T. Sharp.1976. "Mechanics of the Canine Diaphragm." *J. Appl. Physiol.* 41:369-382.

3. Braun, N.M.T.1983. "Force-length Relationship of the Normal Human Diaphragm." *J. Appl. Physiology.: Respirat. Environ. Exercise Physiol.* 55(6):1899-1905.

4. Loring, Stephen H., J. Mead, and N. T. Griscom. 1985. "Dependence of Diaphragmatic Length on Lung Volume and Thoracoabdominal Configuration." *J.Appl. Physiol.* 59(6): 1969-1970.

5. Whitelaw, W. A., L. E. Hajdo, and J. A. Wallace. 1983. "Relationships Among Pressure, Tension and Shape of the Diaphragm." *J. Appl. Physiol.: Respirat. Environ. Exercise Physiol.* 55(6): 1899-1905.

6. Bell, Robert J. T. 1959. Coordinate Geometry of Three Dimensions. London: Macmillan& Co Ltd.

7. Hart, William L. 1963. Analytic Geometry and Calculus. Boston: D.C. Heath and Company.

8. Meyer, Stuant L. 1975. Data Analysis for Scientists and Engineer. New York:John Wiley & Sons.

9. Guest, P. G. 1961. Numerical Methods of Curve Fitting. Cambridge, University Press of University of Sydney, Australia.

10. Bickel, Peter J. 1977. Mathematical Statistics. New York: Holden-Day Inc.

11. The MathWorks. 1989. PC-MATLAB User's Guide.

12. Malcolm, D. 1980. "Interfacial Tension from Height and Diameter of a Single Sessile drop or Captive Bubble." *The Canadian Journal of Chemical Engineering*. 58: 151-153.

13. Langley, L. L. 1974. Dynamic Anatomy & Physiology. fourth edition. New York:McGraw-Hill Book Company.

14. Mountcastle, Vernon B.1968. Medical Physiology. Saint Louis: C. V. Mosby.

## REFERENCES
(Continued)

15. Winton, Frank Robert. 1968. Human Physiology. London: Churchill.

16. Whitelaw, W. A. Personal Communication. September 2, 1993.